

**Stem cell-specific ecdysone signaling regulates the development and function of a  
*Drosophila* sleep homeostat**

Adil R Wani<sup>1</sup>, Budhaditya Chowdhury<sup>2</sup>, Jenny Luong<sup>3</sup>, Gonzalo Morales Chaya<sup>1</sup>,  
Krishna Patel<sup>1</sup>, Jesse Isaacman-Beck<sup>4</sup>, Orie Shafer<sup>2</sup>, Matthew S. Kayser<sup>3,5</sup>#, and  
Mubarak Hussain Syed<sup>1</sup>#

1. Neural Diversity Lab, Department of Biology, University of New Mexico, 219 Yale Blvd Ne, 87131 Albuquerque, NM, USA
2. The Advanced Science Research Center, City University of New York, New York, NY 10031, USA
3. Department of Psychiatry, Perelman School of Medicine at the University of Pennsylvania, Philadelphia, PA 19104, USA.
4. Department of Neurobiology, Stanford University, Stanford, CA 94305
5. Chronobiology Sleep Institute, Perelman School of Medicine at the University of Pennsylvania, Philadelphia, PA 19104, USA.

# Correspondence: [kayser@pennmedicine.upenn.edu](mailto:kayser@pennmedicine.upenn.edu), [FlyGuy@unm.edu](mailto:FlyGuy@unm.edu)

## Abstract

Complex behaviors arise from neural circuits that are assembled from diverse cell types. Sleep is a conserved and essential behavior, yet little is known regarding how the nervous system generates neuron types of the sleep-wake circuit. Here, we focus on the specification of *Drosophila* sleep-promoting neurons—long-field tangential input neurons that project to the dorsal layers of the fan-shaped body neuropil in the central complex (CX). We use lineage analysis and genetic birth dating to identify two bilateral Type II neural stem cells that generate these dorsal fan-shaped body (dFB) neurons. We show that adult dFB neurons express Ecdysone-induced protein E93, and loss of Ecdysone signaling or E93 in Type II NSCs results in the misspecification of the adult dFB neurons. Finally, we show that E93 knockdown in Type II NSCs affects adult sleep behavior. Our results provide insight into how extrinsic hormonal signaling acts on NSCs to generate neuronal diversity required for adult sleep behavior. These findings suggest that some adult sleep disorders might derive from defects in stem cell-specific temporal neurodevelopmental programs.

## Introduction

Proper brain function relies on generating diverse cell types at the appropriate time and place<sup>1</sup>. All neural (neurons and glia) cell types arise from a pool of progenitors called neural stem cells (NSCs)<sup>1–8</sup>. During development, NSCs divide to self-renew and generate distinct classes of neural subtypes over time. These processes are governed by spatial and temporal programs<sup>9–13</sup>. As NSCs age, they express distinct cohorts of genes; this phenomenon is called temporal patterning, allowing individual NSCs to generate distinct progeny over time<sup>1,3–8</sup>. The concept of temporal patterning was first defined in the *Drosophila* embryonic NSCs, which produce simple larval lineages<sup>14</sup>. Later, similar principles were also observed in the *Drosophila* larval NSCs that generate lineages of the adult brain<sup>15–19</sup>, as well as mammalian neural progenitors that generate the retina, spinal cord, and cortex<sup>20–27</sup>. While much is known about the temporal patterning mechanisms of the *Drosophila* NSCs, genetic programs that regulate the formation of the adult central complex (CX) lineages are poorly understood.

The insect CX is a higher-order brain center regulating complex behaviors such as navigation<sup>28–40</sup>, locomotion<sup>29,41–46</sup>, feeding<sup>47,48</sup>, and sleep<sup>49–60</sup>. The CX is a centrally located brain region comprised of four major neuropils: a handlebar-shaped protocerebral bridge (PB), a Fan-shaped body (FB), a doughnut-shaped ellipsoid body (EB), and a pair of noduli (NO)<sup>29,36,61,62</sup>. Two orthogonally arranged neuron types divide the CX neuropil into columns and layers: columnar (small-field) neurons divide the neuropil structure into distinct columns along the anteroposterior axis, and tangential (large-field) neurons send projections and provide input from lateral brain neuropil to the CX<sup>36,61,62</sup>. Recent connectome data has identified ~400 unique neural types in the CX that are thought to be essential in regulating diverse behaviors<sup>36</sup>. How this diversity arises during development is not completely understood.

The neural lineages of the CX are generated by the relatively rare "Type II" NSCs<sup>63–68</sup>. The larval Type II NSCs occupy distinct brain regions and are organized into dorsomedial DM (1-6) and two dorsolateral (DL1-2) groups. Although only sixteen in number, Type II NSCs produce more complex and diverse lineages by generating transit-amplifying intermediate neural progenitors (INPs)<sup>69–71</sup> (Figure 1A). Each Type II NSC produces roughly 40-50 INPs<sup>65</sup>, and each INP divides 4-5 times to produce about ten progeny; hence each Type II NSC is thought to generate approximately 400-500 progeny<sup>63,72</sup>. This division pattern of Type II NSCs is reminiscent of a division pattern of the primate outer radial glia (oRG) that generate lineages containing INPs and make neurons of the cortex<sup>73–76</sup>. Understanding how Type II NSCs produce diverse lineages of the CX might provide insights into understanding the mechanisms that regulate neural diversity in mammals. Additionally, the NSCs that generate most columnar neurons of the CX are conserved in all insects studied to date<sup>77–84</sup>. Thus, understanding how CX neurons are generated in *Drosophila* will likely reveal conserved developmental mechanisms.

Clonal analysis has revealed unique contributions of each Type II NSC to the adult CX neuropil structures<sup>63,64,68</sup>. Among Type II NSCs, four (DM1-4) generate columnar neurons, and DL1 primarily generates long-field tangential neurons of the CX<sup>63,64</sup>. However, DM4 and DM6 also generate some long-field neurons, reflecting diverse

classes of tangential input neurons<sup>63,64</sup>. In addition, each Type II NSCs generates distinct classes of neurons and glia over time<sup>7,15,17,65,67,72</sup>. Temporal clonal analysis has also revealed that INPs generate neurons of diverse identities after each division<sup>7,65,72</sup>, suggesting that Type II NSCs and INPs employ combinatorial temporal programs to diversify CX cell types<sup>7,72</sup>. What programs in Type II NSCs and INPs might regulate the temporally distinct program generating neuronal diversity? In recent studies, the larval Type II NSCs were shown to express a group of transcription factors (TFs) and RNA-binding proteins (RBPs) with precise temporal specificity<sup>15,17</sup>. Young Type II NSCs express early factors Castor, Sevenup, Chinmo, IGF-II mRNA-binding protein (Imp), and Lin-28; later, as NSCs age, they express ecdysone receptor (EcR), Broad, ecdysone-induced protein 93 (E93), and Syncrip<sup>15,17,19</sup>. Interestingly, the temporal expression of EcR around ~55h after larval hatching (ALH) mediates early to late gene transition via NSC extrinsic ecdysone signaling<sup>15</sup>. Thus, unlike embryonic NSCs and larval optic lobe NSCs, generating complex adult lineages requires coordination of both stem cell intrinsic and extrinsic programs<sup>7,15</sup>. However, whether these temporally expressed genes and ecdysone play any role in the fate specification and function of the adult CX neurons is currently unknown. Furthermore, whether these temporal molecular cues regulate adult behaviors has remained unexplored.

Sleep is an evolutionarily conserved behavior essential for numerous physiological functions<sup>60,85,86</sup>. The *Drosophila* CX has repeatedly been implicated as an axis for sleep-wake regulation<sup>50–53,57,58,87–90</sup>. One brain area that has received particular attention is the FB of the CX, where 2310-GAL4 labeled sleep-promoting dFB neurons (subsequently called dFB neurons) innervate and regulate sleep homeostasis. These neurons are classified as long-field tangential input neurons and are about ~12 on each side of the brain<sup>51</sup>. Activation of dFB neurons has been found to increase sleep<sup>50,51</sup> and these neurons are more excitable following sleep deprivation<sup>52</sup>, although recent work has raised questions regarding the precise role of these cells<sup>91,92</sup>. Additionally, young adult flies exhibit increased sleep duration and depth, similar to mammals<sup>54,55,93,94</sup>; dFB neurons appear to play a role in generating this juvenile sleep state<sup>54,55</sup>. Little is known regarding the developmental origin of the dFB sleep neurons. More broadly, while linking sleep

behavior to a unique NSC population is challenging in vertebrates, understanding the development of the sleep-wake circuit is crucial, as many neurodevelopmental disorders arise due to impairments in neurogenesis, circuit formation, and comorbid sleep defects with more fragmented sleep architecture<sup>95–100</sup>.

Here, we focus on the lineage analysis and development of the dFB neurons. Using sophisticated genetics and lineage analysis, we have identified NSCs that generate the sleep-promoting dFB neurons, known to be involved in homeostatic sleep behavior. Specifically, we show that most dFB neurons are born from the dorsolateral1 (DL1) Type II NSC, while 1-2 dFBs are born from the dorsomedial 1 (DM1) NSC. We also show that dFB neurons are generated between 48-76h ALH, and the steroid hormone signaling via E93 specifies dFB neurons. Finally, we show that NSC-specific E93 is required for normal juvenile and mature adult sleep properties. These results demonstrate the developmental origin and birth timing of sleep-promoting neurons and establish the role of steroid hormonal signaling via E93 in promoting sleep architecture.

## Results

### Sleep-promoting dFB neurons are born from Type II NSCs

Most of the neurons and glia derived from Type II NSCs populate the CX – which includes local and long-field tangential input neurons<sup>63,64,68</sup>. We used intersectional genetics to address whether dFB neurons originate from Type II NSCs. We used a Type II NSC-specific flippase (FLP) enzyme to permanently flip out the stop cassette from LexAop-FRT-stop-FRT-mCD8GFP and a cell class marker 23E10-LexA to label dFB neurons in the adult. In this intersectional approach, if the neurons of our interest are derived from Type II NSCs, the neurons will be labeled in green in the adult brain. We expressed FLP in all Type II NSCs using the Wor-GAL4, Ase-GAL80 driver to make the LexAop-FRT-stop-FRT-mCD8GFP reporter functional only in Type II NSCs (Figure 1B). We observed all 12 bilateral sleep-promoting dFB neurons labeled in green (Figure 1C), confirming that all sleep-promoting dFB neurons are derived from Type II NSCs. Thus, we have identified that Type II NSCs generate adult sleep-promoting neurons.

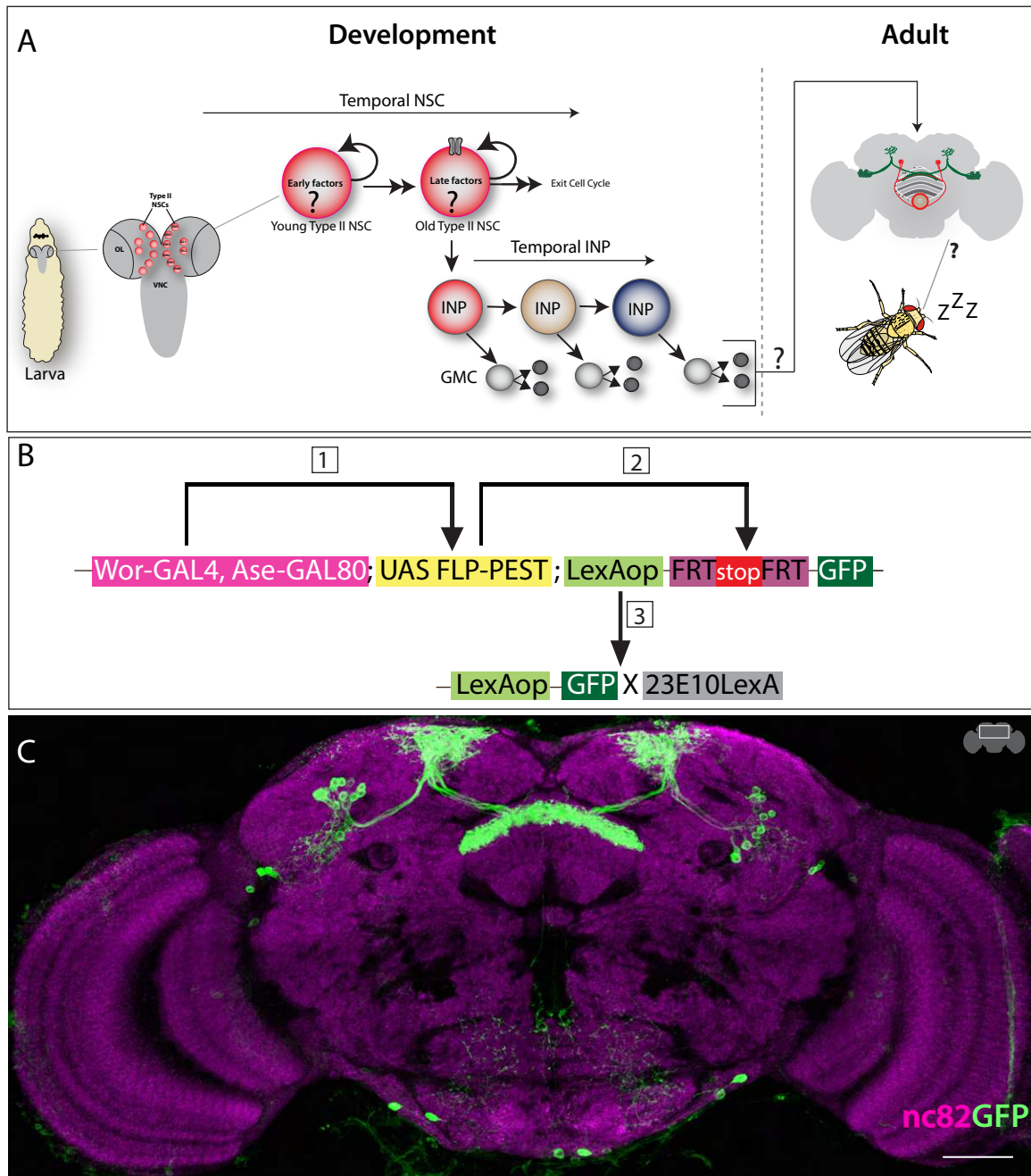


**Figure 1 Sleep-promoting dFB neurons are generated by Type II NSC lineages**

A) Schematics of larval Type II NSCs (8 per lobe: DM1-6, DL1-2), which divide asymmetrically over 120 hours ALH to generate INPs and express early and late TTFs. The temporally expressed EcR mediates the switch from early to late transition. The Type II NSC TTFs and INP temporal factors are thought to contribute to the formation and diversification of neural lineages of the *Drosophila* central complex. We are investigating the role of ecdysone signaling in the specification and function of dFB sleep-promoting neurons, which are part of the *Drosophila* sleep-wake circuit.

B) Schematics showing intersectional genetic strategy for Type II NSC lineage analysis. The Worni-GAL4, Ase-GAL80 combination drives the expression of FLP in all Type II NSCs, which excises a stop and makes LexAopmCD8GFP functional in all Type II NSCs and their progeny. This allows dFB neurons to be labeled in green if produced from Type II NSCs.

C) The FLP expression in Type II NSCs labels all adult dFB neurons (green) (max projection), and nc82 labels neuropil (magenta) (projections showing only FB). The expression of GFP reporter in dFB neurons confirms that they are part of Type II NSC lineages.

Scale bars, 20 $\mu$ m, n = 8 adult brains.

## Two distinct Type II NSCs generate sleep-promoting dFB neurons

Previous studies have assigned a unique clone morphology to each NSC present in the larval central brain, thus providing a reference framework for the clonal developmental organization of the adult *Drosophila* brain<sup>63,64,68</sup>. The DM1-4 Type II NSCs generate most local columnar neurons, and DL1 generates the majority of long-filed tangential input neurons with a minor contribution from DM4 and 6<sup>63,64,101</sup>. To determine which Type II NSCs generate dFB neurons, we used a heat shock-based lineage filtering method called cell class-lineage analysis (CLIn)<sup>102</sup>. This lineage filtering method classifies Type II NSC lineages by assigning cells to specific categories based on the clone morphology and connectivity patterns<sup>102</sup>. Using CLIn, one can generate individual Type II NSC clones by giving a temporal heat shock during development. In a successful flip-out event, the entire lineage of the Type II NSCs is labeled in red (reporter A). At the same time, the specific neuronal type marked by the GAL4 will be labeled with the GFP (reporter B) (Figure 2A, 2B).

We adopted CLIn genetic strategy, induced a 10–12-minute heat shock at 0h ALH, and analyzed individual Type II NSC clones labeled in red (mCherry) in the adult brain (see methods for detailed protocol). Using this method, we generated single Type II NSC clones, and these individual clones were used to assign lineages to the dFB neurons. Individual clones were confirmed by comparing the reporter images with the previously published clonal map<sup>63,64,68</sup>. Interestingly, we observed that most dFBs (~10) are derived from DL1 (Figure 2C), but ~1-2 neurons are generated by DM1 Type II NSC (Figure 2D). The mixed lineage assignment of the dFB neurons to DL1 and DM1 Type II NSCs indicates heterogeneous cell types within the dFB cluster. Previous clonal studies might have missed DM1 contribution in generating long-field tangential neurons since they have not assigned these neuron types to the DM1 lineages (see discussion).

## Sleep-promoting dFB neurons are generated by late Type II NSCs

Type II NSCs express different classes of genes in the early and late portions of their lineage, which are thought to regulate the identity of the neurons born in their expression window<sup>6,7,15,17,103</sup>. We wanted to determine whether dFB neurons are born from early or

late Type II NSCs. To identify the birth timing of the dFB neurons, we performed genetic birthdating by utilizing the heat shock-based CLIn method, as discussed above, but we performed multiple heat shock events at different times during larval development. Briefly, we crossed 23E10-GAL4, which labels dFB neurons, to the CLIn fly (for genotype, see STAR table) and gave heat shock to the progeny at three major development time points: 0h, 48h, and 76h ALH (Figure 2E). There are two phases of neurogenesis, embryonic and larval<sup>1,6,7,104–106</sup>. While most embryonic-born neurons die during metamorphosis<sup>107–112</sup>, a small population survives, undergoes metamorphosis<sup>111,113,114</sup>, and contributes to the adult brain<sup>114–117</sup>. The neurons and glia generated in the larval phase of neurogenesis predominantly contribute to adult brain circuits<sup>63,64,68,118</sup>. When we performed 0h ALH heat shock, we observed all the dFB neurons labeled in the adult brain, confirming that all dFB neurons are generated post-embryonically (Figure 2F). Next, we wanted to narrow down their birth time precisely to the time they are derived from Type II NSCs and performed heat shock at 48h and 76h ALH. Upon analyzing the dFB neurons in the adult brain, we observed that most dFB neurons were labeled in 0h and 48h ALH heat-shocked larvae (Figure 2F, G). However, when 76h ALH heat-shocked larvae were analyzed, we did not observe any labeled dFB neurons in the adult brain, confirming that most dFB neurons are born between 48h and 76h ALH (Figure 2E-H). Taken together, we conclude that sleep-promoting dFB neurons are born from late DL1 and DM1 Type II NSCs—at the time of EcR-mediated temporal gene expression<sup>15</sup>.

### **Ecdysone signaling in Type II NSCs is required for dFB neuronal fate**

The insect growth hormone Ecdysone regulates various stages of nervous system development, including neurogenesis, refining neural connections through pruning, and regulating programmed cell death<sup>110,111,113,119–122</sup>. In *Drosophila*, Ecdysone is present in varying concentrations throughout development<sup>111,120,123</sup>; however, Type II NSCs express EcR temporally, which transduces the extrinsic hormonal signal into the cell to regulate temporal gene expression<sup>15</sup>. To investigate the role of Type II NSC-specific EcR in dFB fate specification, we generated EcR-FLPStop2.0 transgenic fly. FLPStop2.0 is a modified and efficient version of the conditional loss of function strategy using the FlipStop technique<sup>124</sup> (Figure 3A) with an added repeated ribozyme motif known to disrupt

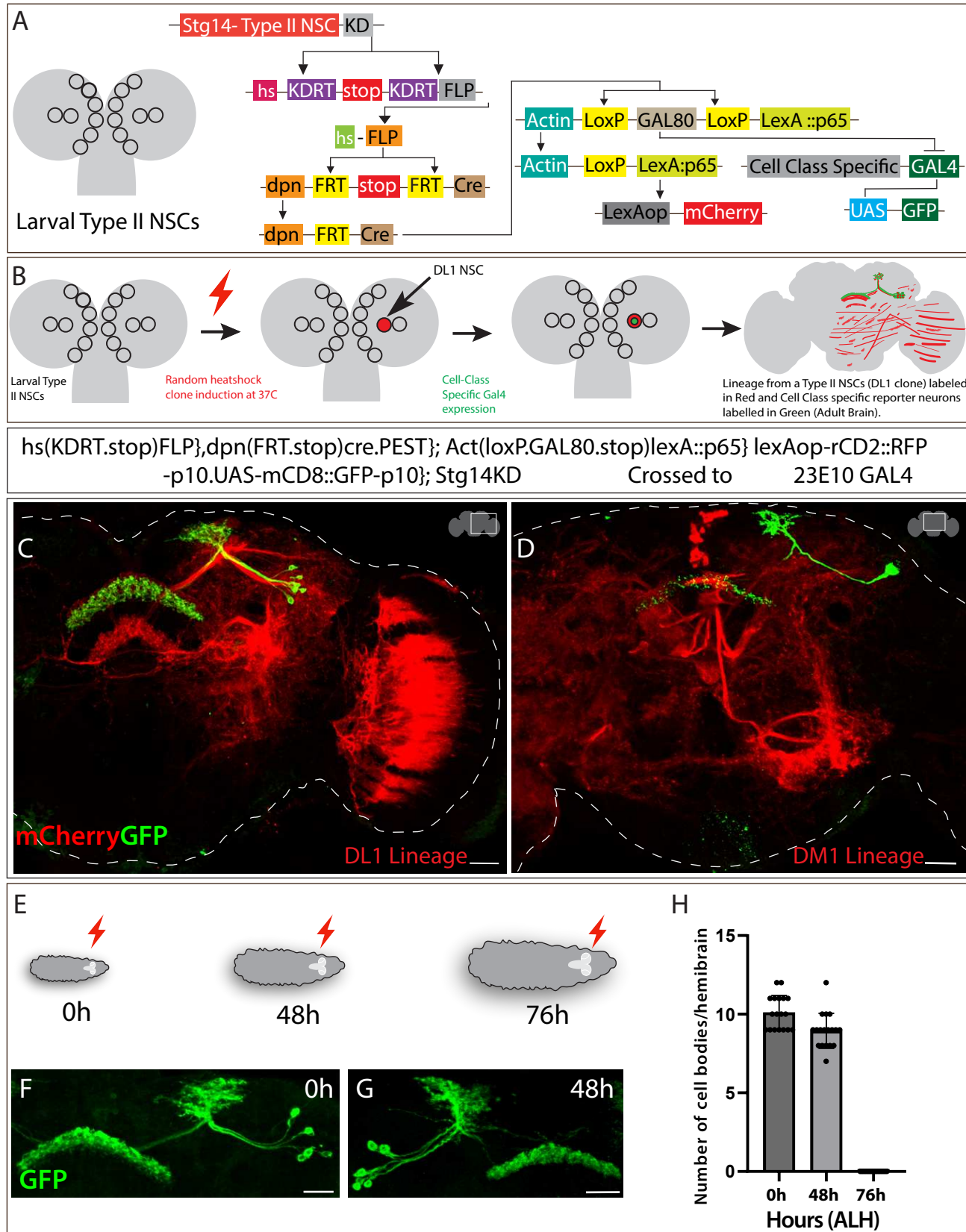


## Figure 2 Sleep-promoting dFB neurons are generated by late DL1 and DM1 Type II NSCs

A) Schematics of CLIn intersectional genetics explaining how different genetic elements work in a sequence to label different Type II NSC lineages. The CLIn flies use Type II NSC-specific promotor, *stg*, to express KD recombinase in Type II-specific manner. The KD recombinase removes the stop sequence, bringing the FLP in frame with the heat shock promotor only in Type II NSCs. The FLP expression removes the stop sequence upon heat shock, making Cre recombinase active in Type II NSCs. The Cre recombinase makes LexA::p65 functional, making the lineage-specific expression of reporter mCherry possible. The removal of GAL80 by Cre recombinase also removes the inhibition of GAL4, making the expression of mCD8GFP in a class-specific manner.

B) Schematics of how CLIn allows lineage analysis of Type II NSCs. The stochastic heat-sensitive FLP event in a single Type II NSC labels all neurons and glia born from that particular NSC.

C) Single DL1 NSC clone induced at 0h ALH labels most dFB neurons (green). All the lineages from DL1 NSC are labeled in red (mCherry) and dFB neurons in green.

D) Single DM1 NSC clone induced at 0h ALH labels 1-2 dFB neurons. The DM1 lineages are labeled in red (mCherry), and dFB neurons in green.

E) Schematics representing heat shock given at different time points during larval development. The red lightning bolt symbol indicates heat shock given at three different time points 0h, 48h, and 76h after larval hatching (ALH).

F-H) Clones induced at 0h and 48h ALH label all the dFB neurons (F, G), while clones induced at 76h ALH didn't label any dFB neurons (not shown)

H) Quantification of dFB neuron cell bodies labeled per hemibrain when clones are induced at 0h, 48h, and 76h ALH.

Scale bars, 20 $\mu$ m, n = 16 adult hemibrains.

expression<sup>125</sup> (Figure 3A, Star Methods). This method was needed due to the failure of EcR-RNAi to knock down EcR levels in Type II NSCs (data not shown). In the FLP-Stop method, tissue-specific FLP recombinase expression inverts the cassette, which results in a premature stop; as a result, a conditional loss of function allele is generated (Figure 3A). Upon this inversion, the fluorescent tag UAS-tdTomato becomes functional and labels mutant cells in red color<sup>124</sup> (Figure 3A). To check whether EcR-FLPStop2.0 abolishes the EcR function, we expressed FLP in Type II NSCs by crossing Pointed-GAL4 to UAS-FLP in the EcR-FLPStop 2.0 background. We also added lineage tracing cassette Act-FRT-stop-FRT-GAL4 to trace mutant lineages to the adult brain (see star tables genotype). In the progeny with the genotype UAS-FLP, Act-FRT-Stop-FRT-GAL4; UAS-EcR-FLPStop2.0/Pointed-GAL4, all the EcR loss of function progeny were labeled in red, and we observed a significant reduction of EcR and E93 protein in Type II NSCs and their progeny (Figure 3S1 A-B'), confirming that EcR-FLPStop2.0 severely reduces EcR function. In the EcR-FLPStop2.0 background, we used 23E10-LexA, LexAop-mCD8GFP to label dFB neurons in green. In the progeny with the genotype UAS-FLP, Act-FRT-stop-FRT-GAL4; UAS-EcR-FLPStop2.0, 23E10-LexA; Pointed-GAL4, LexAop-mCD8GFP, we were able to simultaneously create EcR loss of function in Type II NSCs and label dFB neurons in the adult. We examined whether loss of EcR in Type II NSCs leads to defects in the specification, morphology, or connectivity of the dFB neurons. There are ~12 dFB neurons on each side of the brain, with cell bodies located in the exterior of the CX in the PPL region. These neurons send the axonal projections to layer 6 of the dorsal FB, where they are thought to connect with the helicon cells to regulate sleep homeostasis<sup>51</sup>. In most experimental flies, depletion of EcR in Type II NSCs resulted in the loss of dFB neurons in the adult brain (Figure 3C-D'), suggesting that ecdysone signaling in Type II NSCs is necessary for the formation of dFB neurons.

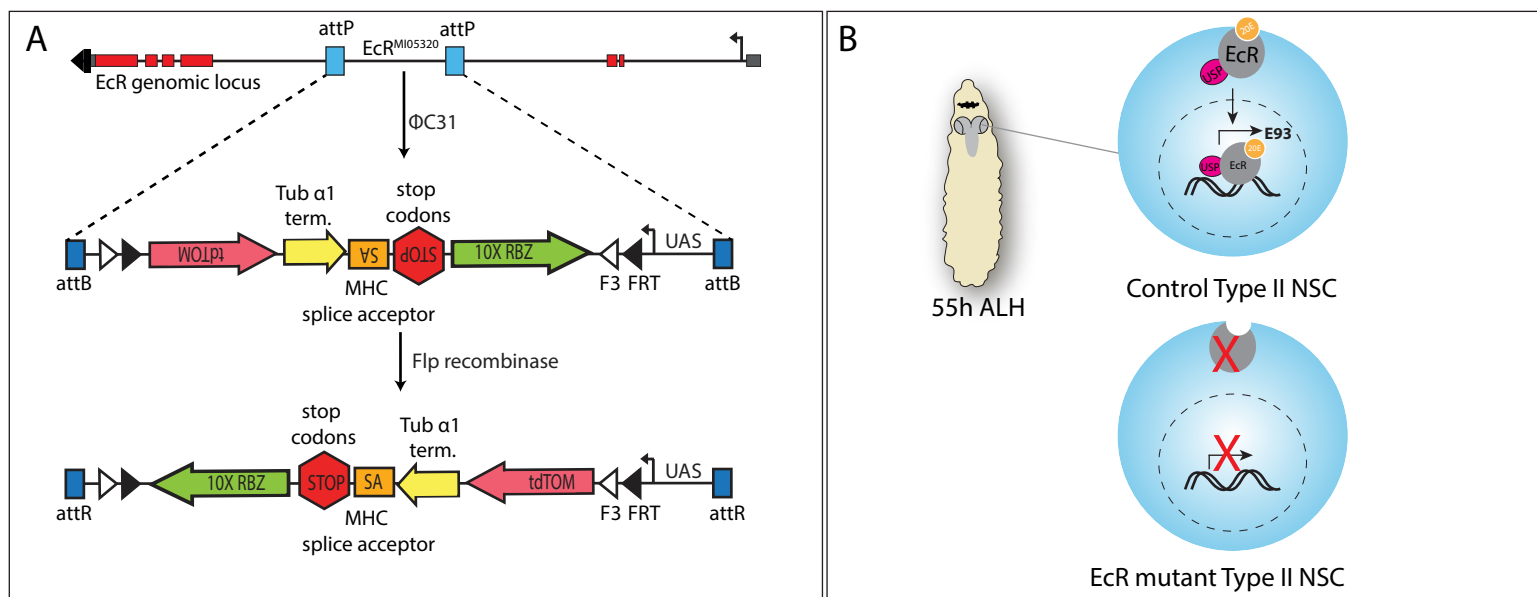
To further investigate whether the steroid hormone ecdysone regulates the dFB fate and connectivity, we use EcR dominant negative (DN)<sup>126</sup> to block the ecdysone signaling. We specifically blocked ecdysone signaling in larval Type II NSCs by expressing EcR-DN with Pointed-GAL4 and assayed the fate of dFB neurons in the adult brain. We found that blocking ecdysone signaling in Type II NSCs affects dFB fate, similar to the EcR loss of

function (Figure 3 E, E'). In EcR loss of function animals, we also found some animals with a less penetrant phenotype, where a few neurons were present (Figure 3F-G'); however, interestingly, the connectivity of the surviving neurons was severely disrupted (Figure 3G, G'). Compared to the control brains (Figure 3F-F'), where dFB neurons send their axonal projections to layer 6 of the dorsal portion of the fan-shaped body, in EcR loss of function (Figure 3G-G'), surviving neurons ectopically project to the ventral layers of the FB. A similar mistargeting phenotype was observed in the surviving dFB neurons in EcR dominant negative experimental animals (Figure 3H, H'), indicating multiple roles of EcR and ecdysone signaling in specifying sleep-wake circuit (see discussion). Taken together, our findings suggest that Type II NSC-specific ecdysone signaling is essential for the proper formation and identity of the dFB neurons (Figure 3I). Upon misexpression of EcR in Type II NSCs throughout development, we did not observe any increase in the dFB numbers (Figure 3S2 A-C), indicating that EcR alone might not be sufficient for generating dFB neuron types. Taken together, our studies link an extrinsic hormonal signal to the NSC-intrinsic gene programs via temporal expression of EcR in late NSCs to generate sleep-promoting neurons.

Using nc82 staining, we also investigated whether EcR in Type II NSCs regulates the overall architecture of CX neuropil structures—PB, FB, EB, and NO. Interestingly, the adult EB structure was defective upon EcR loss of function in Type II NSC lineages (Figure 3S3 A-B'). The EB did not fuse appropriately in the experimental flies, and there was a cleft in the posterior EB. We did not observe any severe morphological defects in the other neuropil structures, suggesting that ecdysone signaling regulates the fate of CX neuronal subtypes, in particular dFB neurons (Figure 3S3 A-B'). To our knowledge, these findings are the first to relate the extrinsic ecdysone signal to stem cell intrinsic gene programs to specify sleep-promoting neurons and CX development.

### **Ecdysone signaling in Type II NSCs governs dFB neuronal fate via E93**

Next, we wanted to understand how Type II NSC-specific ecdysone signaling regulates dFB neuronal specification. Our previous work identified ecdysone signaling as the primary regulator of early to late gene transitions in Type II NSCs<sup>15</sup>. Around ~55 ALH,



23E10-LexA ; Pointed-GAL4, LexAop-mCD8GFP

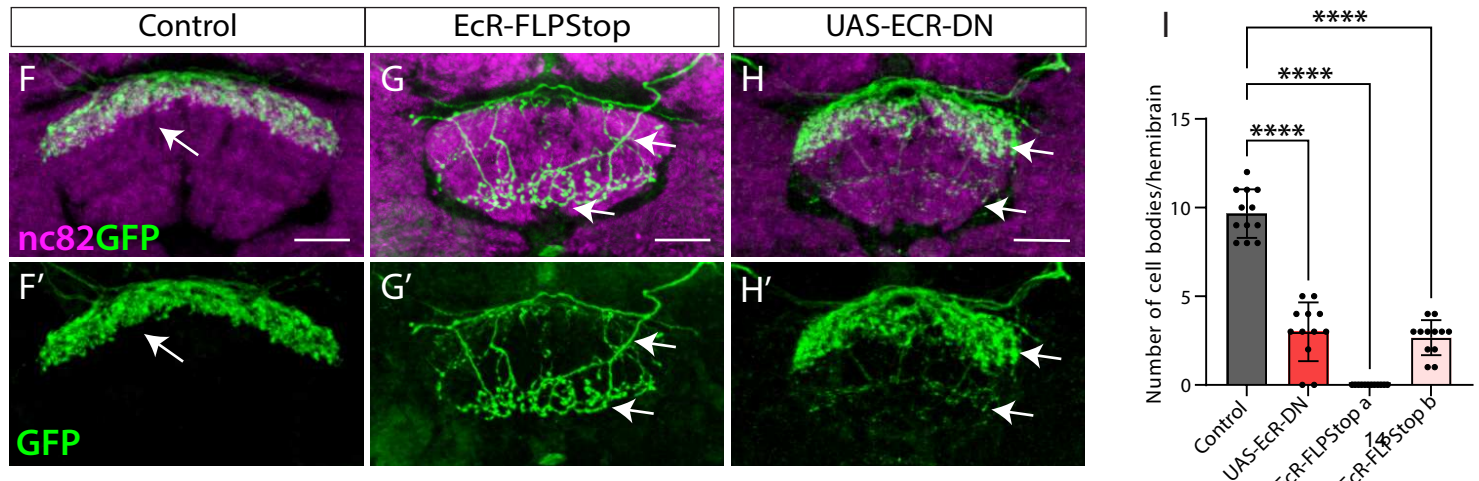
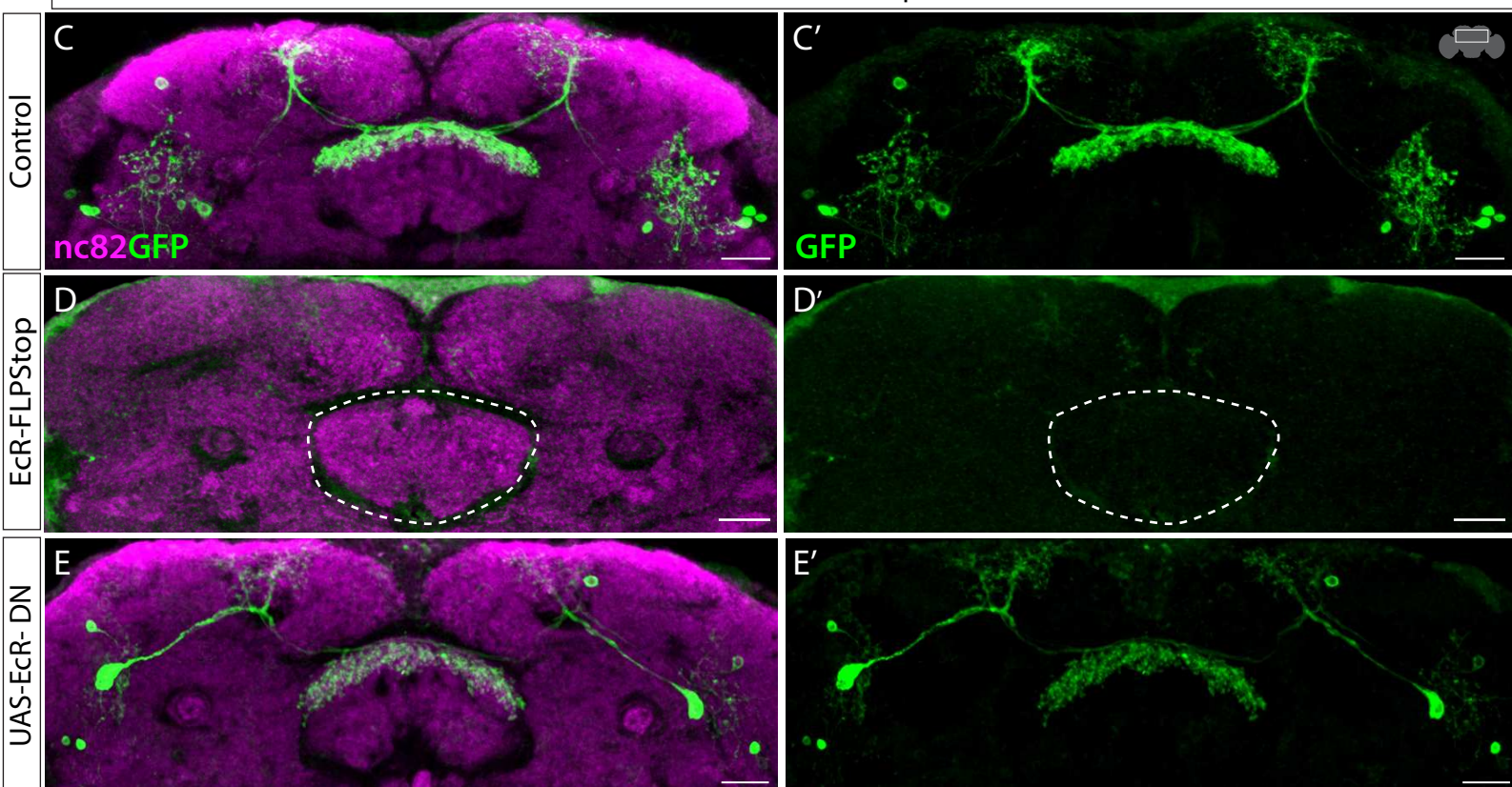


### Figure 3 Ecdysone signaling regulates dFB neuron specification

A) Genetic elements of EcR-FlpStop2.0 scheme. The expression of FLP recombinase in Type II NSCs flips the tdTomato sequence in frame with a UAS promoter, allowing it to label mutant cells specifically under the control of the Type II specific GAL4 in red color. The FLP event also inverts the STOP sequence - transcription-based disruption (Tub $\alpha$ 1 terminator and 10x Ribozyme sequence) and translation disruption (MHC splice acceptor paired with STOP codons) - to generate a premature stop, disrupting EcR expression and function.

B) Schematics showing typical Type II NSC expressing EcR at 55h ALH that leads to expression of other EcR-induced downstream genes; upon removal of ecdysone receptor, the expression of target genes is disrupted.

C, C') Shows a control brain with GFP-labeled dFB neurons and their projection pattern in the FB.

D, D') Upon EcR loss of function in Type II NSCs, dFB neurons are not specified (dashed line annotates the FB).

E, E') Blocking ecdysone signaling in Type II NSCs using EcR-DN results in significant loss of dFB neurons.

F-H') In control brains, the dFB neurons project to layer 6 of the FB (F, F'); in EcR loss of function (G, G') and EcR-DN (H, H') animals, the surviving dFB neurons miss target to the ectopic FB layers indicated by arrows.

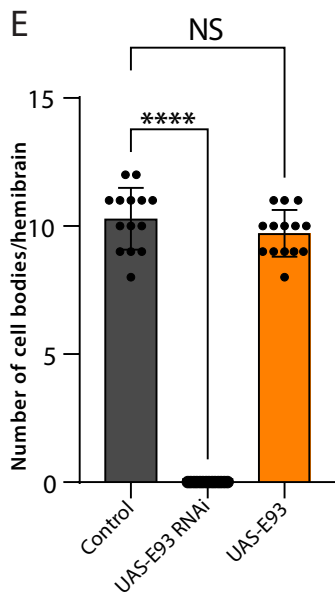
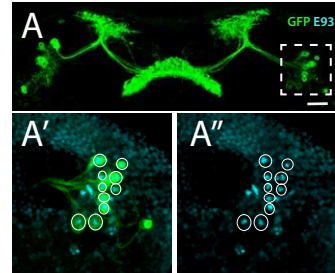
I) One-way ANOVA test quantification of dFB neuron cell bodies. Error bars represent SEM; \* p<0.05, \*\*p<0.01, \*\*\*p<0.001, \*\*\*\* p<0.0001, NS, non-significant.

Scale bars, 20 $\mu$ m, n = 10 adult hemibrains.

temporal expression of EcR in Type II NSCs activates late genes (Figure 1A), which includes the Ecdysone-induced gene, E93. Interestingly, all sleep-promoting dFB neurons express E93 in their cell bodies, indicating that EcR might specify dFB fate via E93 (Figure 4A-A’). To test this hypothesis, we used Pointed-GAL4 to knock down E93 in all Type II NSCs during development and assayed dFB neurons labeled with 23E10-LexA, LexAop-mCD8GFP in adults. We confirmed the efficiency and specificity of UAS-E93RNAi by staining larval Type II NSCs for E93 expression (Figure 4S1). For the control experiments, we crossed Pointed-GAL4 to an empty RNAi, UAS-KKRNAi, which has the same genetic background as UAS-E93RNAi (see methods). Compared to the controls (Figure 4B-B’), reducing E93 levels in Type II NSCs resulted in the absence of all dFB neurons (Figure 4C-C’), quantified in (Figure 4E), confirming that late Type II specific E93 expression is essential for the specification of dFB neurons. In the experimental flies, we noticed 2-3 cell bodies were always present; however, we observed them in the controls as well, and these neurons are not part of the dFB cluster since they do not send projections to the dorsal fan-shaped body. Taken together, we conclude that the late temporal expression of E93, activated by EcR, regulates the formation of adult dFB neurons. To ensure the phenotype is E93 specific, we further confirmed our results using E93 RNAi without dicer and an additional independent E93 RNAi line (Figure 4S2 A-C; see STAR Methods). Both conditions produced similar phenotypes; however, E93 RNAi with dicer produced a more severe phenotype (Figure 4S2 A-C). Unlike EcR loss of function, E93 knockdown in Type II NSCs did not affect the morphology of the adult CX neuropil (including EB) (Figure 4S3 A-C’), suggesting that E93 is not essential for the overall CX neuropil development and specifically regulates dFB neuronal fate.

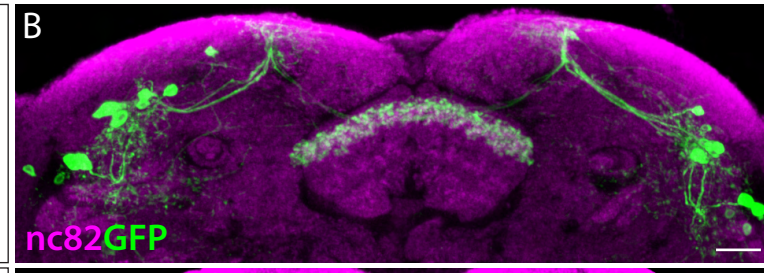
Next, we wanted to test whether E93 is sufficient to specify dFB neurons. We used Pointed-GAL4, UAS-E93 to miss express E93 in Type II NSCs throughout larval development and 23E10-LexA, LexAop-mCD8GFP to label dFB neurons. Compared to the control (Figure 4B-B’), we did not observe any extra dFB neurons in experimental animals (Figure 4D-D’), quantified in (Figure 4E), indicating that E93 is not sufficient to generate the dFB neuronal fate and rather a combination of factors might be involved.

23E10-GAL4, UAS-mCD8GFP

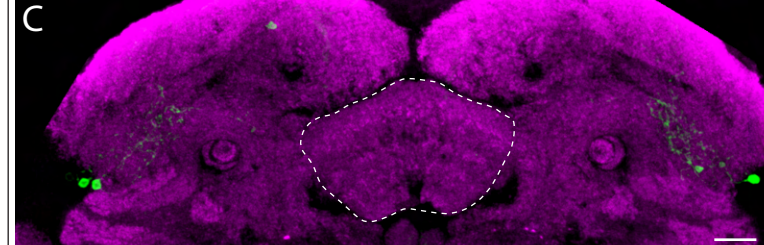


23E10LexA ; Pointed-GAL4, LexAop-mCD8GFP

Control



UAS-Dicer ;  
UAS-E93RNAi



UAS-E93

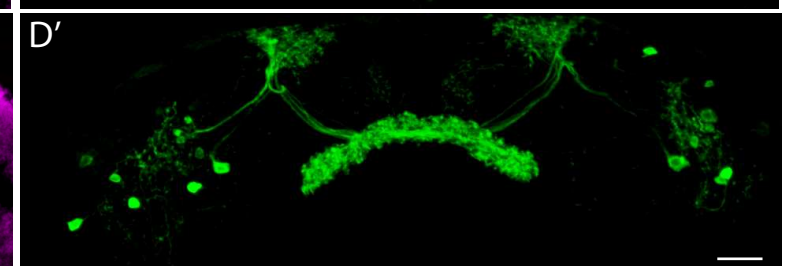
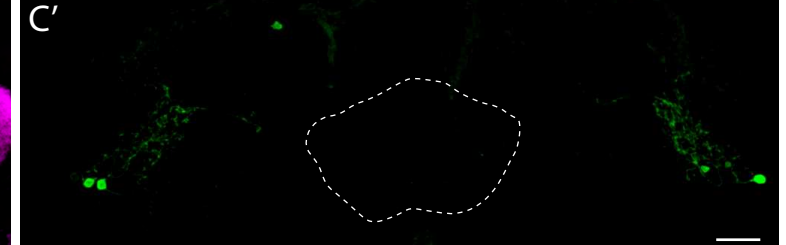
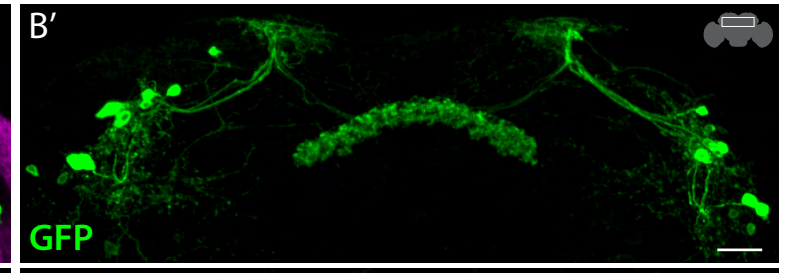
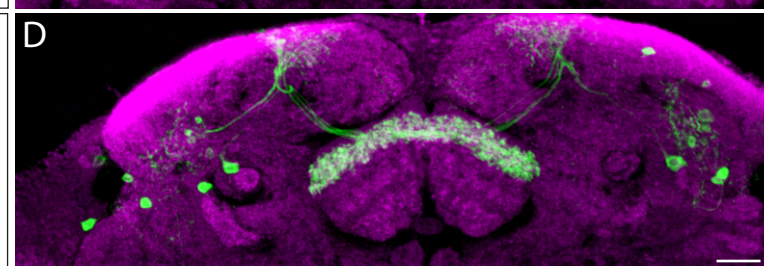


**Figure 4 Ecdysone signaling regulates dFB neural fate specification via E93**

A-A'') The dFB neurons labeled in green (A) express E93 in cell bodies (A', A'').

B, B') Control dFB neurons project normally to the FB.

C, C') Complete loss of dFB neurons upon E93 knock-down in Type-II NSCs.

D, D') No change in cell body number and morphology of dFB neurons upon E93 overexpression in Type-II NSCs.

E) One-way ANOVA test quantification of dFB neuron cell bodies per hemibrain. Error bars represent SEM; \* p<0.05, \*\*p<0.01, \*\*\*p<0.001, \*\*\*\* p<0.0001, NS, non-significant. Scale bars, 20 $\mu$ m, n = 14 adult hemibrains.

Type II NSCs express EcR beginning around ~55h ALH; E93 expression starts right after this developmental time point at a low level, which peaks around pupal formation at 120h ALH<sup>15</sup>. Next, we aimed to narrow down the developmental timing of the E93 function. Since dFB neurons are born between 48-76h ALH, we used the temporal and regional gene expression targeting (TARGET) system<sup>127</sup> to restrict the E93 knockdown during that specific developmental time window (Figure 5A, B). Briefly, at the permissive temperature (18C), GAL80ts is active and inhibits GAL4 activity by binding to its activation domain; this inhibition is lost upon temperature shift to 29C, which allows GAL4 to function (Figure 5A). The knockdown of E93 at 48h ALH or later significantly decreased total dFB neuron number and recapitulated the phenotype observed with constitutive E93 knockdown (Figure 4C-C'), confirming that temporal expression of E93 in Type II NSCs between 48h – 76h ALH is essential for specifying dFB neurons. For the control experiment, we used UAS-E93RNAi without GAL80ts, UAS-E93RNAi; or GAL80ts constitutively grown at 29C and 18C (Figure 5C-F'). The analysis and quantification of control and experimental animals (Figure 5G) suggest that ecdysone-induced, Type II NSC specific temporal E93 expression between 48h-76h ALH specifies dFB neurons.

### **Loss of E93 in larval NSCs impairs adult sleep behaviors**

The *Drosophila* CX has been implicated as a center for sleep regulation<sup>36,50–53,58–60,88–90</sup>, with evidence of a specific role for the dFB in sleep homeostasis<sup>52,87</sup>. We tested if loss of E93 in Type II NSCs affects sleep in adulthood. E93 knockdown in Type II NSCs using Pointed-GAL4 had a very mild effect on total sleep duration in mature adults (Figure 6A), despite dramatic effects on the dFB neuronal fate. Compared to both parental controls, there was a small reduction in daytime sleep duration and no consistent change during the night (Figure 6A). This finding is consistent with studies showing that dFB inhibition has little impact on sleep duration in mature adulthood<sup>55,92</sup>. We did, however, observe a substantial impact on sleep fragmentation during night, with an increase in sleep bout number (Figure 6B) and a decrease in bout length (Figure 6C) in E93 RNAi flies compared to both controls. Recent evidence indicates that sleep in *Drosophila* is not a homogenous state and that deeper sleep occurs during periods of consolidated sleep consisting of long sleep bouts<sup>128–134</sup>. We next asked if long bouts of sleep (60 minutes or longer) might be

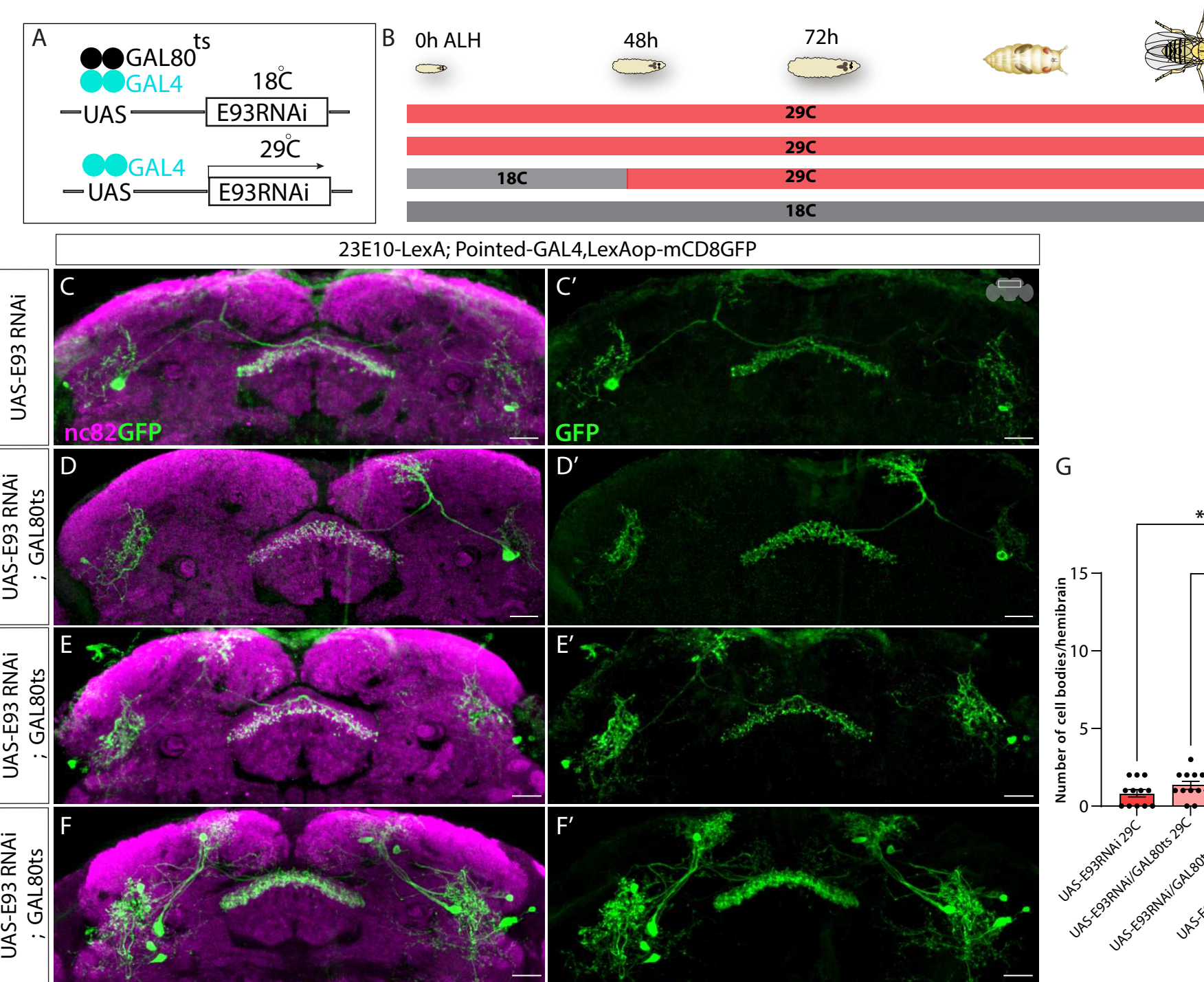


**Figure 5 E93 expression in a restricted time window regulates dFB neuronal fate.**

A) Schematics of TARGET system showing GAL80ts mediated restricted knockdown of E93. At 18°C, GAL80ts will be active, preventing the expression of E93RNAi by inhibiting Pointed-GAL4. At higher temperatures, 29°C, GAL80ts will be inactive, allowing the expression of E93RNAi temporally.

B) Schematics of the experimental setup showing E93 RNAi flies growing at different temperatures and under different conditions across the larval life cycle from 0h ALH to 120h ALH. The E93RNAi experimental flies containing GAL80ts were initially grown at 18°C and later shifted to 29°C around 40h ALH to make E93 RNAi expression possible in late Type II NSCs.

C, C') Shows loss of dFB neurons labeled with GFP at 29°C upon E93 knockdown (E93 RNAi without dicer) D, D') Loss of dFB neurons can be seen upon E93 RNAi combined with Gal80ts grown continuously at 29°C (GAL80ts will be inactive at 29°C)

E, E') Significant loss of dFB neurons can be seen when the UAS-E93 RNAi was restricted to the late Type II NSCs using GAL80ts; the flies were grown at 18°C till 40h ALH and then shifted to 29°C to make GAL80ts inactive.

F, F') The dFB neuron number is normal when flies expressing UAS-E93RNAi combined with Gal80ts are grown continuously under 18°C.

G) One-way ANOVA test quantification of dFB neuron cell bodies per hemibrain. Error bars represent SEM; \* p<0.05, \*\*p<0.01, \*\*\*p<0.001, \*\*\*\* p<0.0001, NS, non-significant. Scale bars, 20μm, n = 12 adult hemibrains.

selectively affected by E93 knockdown; our analysis focused on the night period since this is when deep sleep primarily occurs<sup>128,130,131</sup>. Indeed, we found a marked reduction in the duration of sleep comprised of long sleep bouts in the night with E93 knockdown compared to controls, suggesting a role for the dFB in deep sleep (Figure 6S1).

During juvenile developmental periods across species, including early adulthood in *Drosophila*, sleep depth (and duration) are elevated<sup>54,55</sup>. Juvenile flies (Day 1 post eclosion) exhibit increased arousal threshold during the day and night compared to mature adults (Day 5-9) and an increase in sleep duration during the day period<sup>54,55</sup>. We next investigated if the knockdown of E93 in Type II NSCs affects juvenile adult sleep. We found that expression of E93 RNAi was associated with a reduction in total daytime sleep duration in juvenile adults compared to controls, with no impact on sleep time during the night (Figure 6D). However, sleep was more fragmented across day and night (Figure 6E, F), as evidenced by increased sleep bout number and reduced bout length (Figure 6E,F). These results suggest a particular sensitivity of juvenile sleep to the loss of sleep-promoting dFB neurons.

Finally, we examined how knockdown of E93 in Type II NSCs affects sleep rebound following a night of sleep deprivation in mature adult flies, which is another high sleep pressure state. Total sleep duration during the rebound period (first 6 hours of the morning) was modestly reduced in Pointed-GAL4 > E93 RNAi flies (Figure 6G) but sleep during this period was more fragmented (shorter sleep bouts) (Figure 6H, I). Notably, recent work has raised the possibility that sleep relevant neurons labeled by the 23E10 driver reside in the ventral nerve cord (VNC) rather than (or in addition to) neurons in the brain<sup>91,92</sup>. We found that E93 knockdown in Type II NSCs impairs brain dFB neurons but spares the 23E10+VNC neurons (Figure 6S2). Our developmental approach thus assigns the brain-specific sleep roles for dFB neurons. Specifically, behavioral findings support a role for 23E10+ dFB neurons in promoting consolidated sleep in situations associated with high sleep pressure.

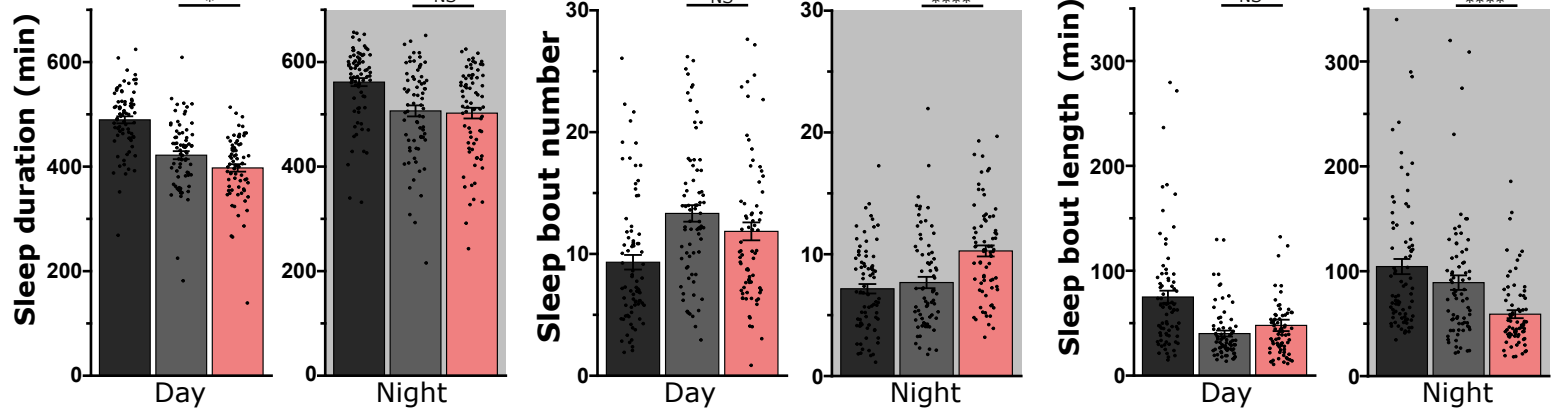
## Mature (D6-8)

bioRxiv preprint doi: <https://doi.org/10.1101/2023.09.29.560022>; this version posted October 2, 2023. The copyright holder for this preprint (which was not certified by peer review) is the author/funder, who has granted bioRxiv a license to display the preprint in perpetuity. It is made available under aCC-BY-NC-ND 4.0 International license.

A

B

C

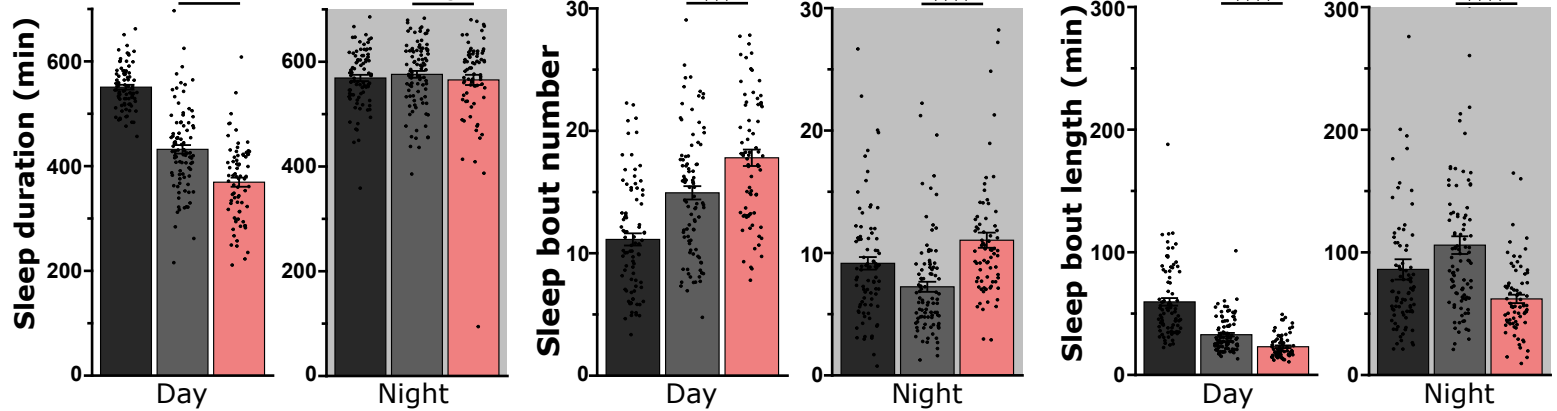


## Juvenile (D1)

D

E

F



## Sleep rebound, Mature (D6-8)

G

H

I

### Genotype

- +/E93-RNAi
- pointed-Gal4 > RNAi control
- pointed-Gal4 > E93-RNAi

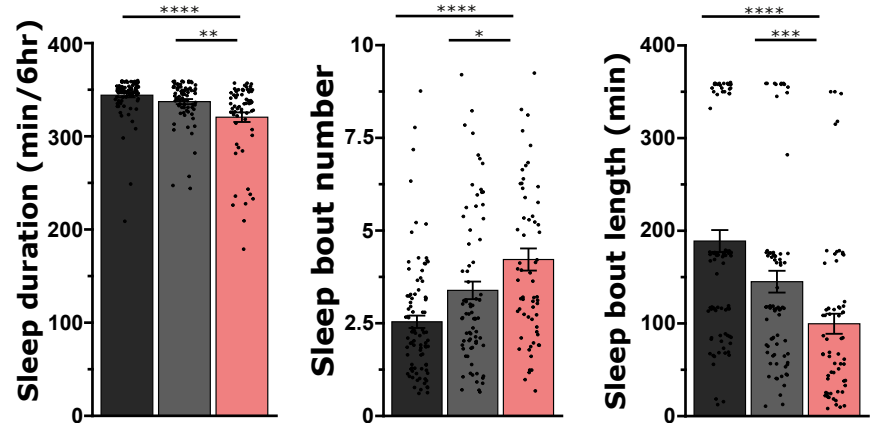


**Figure 6 Knockdown of E93 in larval Type II NSCs impairs adult sleep.**

Quantification of day and night sleep duration (A), sleep bout number (B), and sleep bout length (C) in mature adult flies expressing E93-RNAi under control of pointed-GAL4 (red) compared to genetic controls (black, gray). n=79,74,74 from left to right. Quantification of sleep duration (D), sleep bout number (E), and sleep bout length (F) in juvenile adult E93-RNAi flies and controls. n=85,94,74 from left to right. Quantification of sleep duration (G), sleep bout number (H), and sleep bout length (I) in mature adult E93-RNAi flies and controls over 6 hours following a night (12 hours) of sleep deprivation. n=93,82,67 from left to right.

Error bars represent SEM; \*p<0.05, \*\*p<0.01, \*\*\*p<0.001, \*\*\*\*p<0.0001, NS, non-significant by One-way ANOVA with Mann-Whitney multiple comparisons test corrections.

## Discussion

Generating complex behaviors requires the integration of various sensory modalities to generate motor output in a context-dependent manner. Distinct neuronal cell types provide unique sensory inputs or modulate motor outputs to regulate behaviors such as navigation, feeding, and sleep. Understanding brain function thus requires investigating developmental programs that establish circuits and behaviors. Here, we have investigated the lineage-specific development of sleep-promoting neurons that are an essential part of a sleep-wake circuit<sup>51,53</sup>. Our studies have identified the NSCs that generate dFB sleep-promoting neurons of the brain and mapped their birth timing (Figure 2C, 2D). Our work has identified the crucial role of temporal steroid hormonal signaling in regulating the specification of the dFB neurons via E93 (Figure 4). Furthermore, we identified the role of E93 in Type II NSCs in regulating juvenile and mature adult sleep (Figure 6). This study provides a new perspective on the genetic and developmental basis of sleep, and links sleep behavior to distinct NSCs.

## Lineages to sleep circuits

Diverse classes of large field input neurons feed sensory information to the CX by innervating and making connections in the different layers of the FB. Recent connectome data has specified the distinct modules in the FB layers to specific behaviors, with layers 6-7 as a sleep-wake module<sup>36</sup>. The FB is the most diverse structure of the CX neuropils, which receives input from the periphery via the long-field neurons that innervate different FB layers topographically. The FB long-field neurons arise from diverse NSCs, with significant contributions from the DL1 Type II NSC and DALc12v Type I NSC<sup>63,64,68,101</sup>. The sleep-promoting dFB neurons are long-field input neurons that innervate layers six-seven of the FB<sup>36</sup>. What NSC populations make the long field tangential input neurons of the sleep-wake circuit? Is the lamination of the FB birth order related? Here, we show that the dFB neurons are born from Type II NSCs, while the majority are derived from the DL1 lineages; a few are born from the DM1 lineage. Previous clonal studies could not find any contributions of DM1 lineage to the long-field input neurons. However, consistent with our findings, a recent connectomics-based lineage assignment study has also proposed DM1 lineage contribution to the FB tangential input neurons<sup>101</sup>. Although all ~12 neurons look

similar in morphology, our clonal analysis data suggests a likely heterogeneity of cells in this cluster. It could be each neuron in that cluster is a unique neuron type getting inputs from distinct upstream neurons and part of unique circuits. The connectomic-based studies will help in assigning unique input and output neurons to these distinct classes of dFB neurons. Furthermore, single-cell RNA-Sequencing will help delineate the distinct cell types in the dFB cluster.

Are the neuron types innervating distinct FB layers specified at different times during development? Our findings reveal that the sleep-promoting dFB neurons are born from the old Type II NSCs between 48-76h ALH. Previous studies indicate that large field tangential input neurons that innervate ventral FB layers are generated only until 72h ALH, indicating the time-dependent lamination of the FB<sup>17,135</sup>. Once specified, the dFB neurons innervate the FB around 48h APF where they intermingle with arousal promoting dopaminergic inputs, a process regulated by post-mitotic expression of the conserved gene *pdm3*<sup>56</sup>. Further studies focusing on more neural cell types innervating distinct layers and functioning in discrete neural circuits will be essential to relate time and temporal factors expressed in Type II NSCs with the assembly of the circuits in distinct FB layers.

### **Hormonal regulation of the neural fate**

Our study demonstrates ecdysone signaling via E93 specifies an essential cell type of the sleep-wake circuit, thereby establishing the role of developmental hormonal signaling in specifying sleep-promoting neurons and sleep behavior. These are interesting findings that relate an extrinsic hormonal signal to the stem-cell-intrinsic factors specifying neural fate. Ecdysone signaling plays many roles during development, metamorphosis, and post-development in regulating various physiological processes<sup>110,111,136,137</sup>. Although ecdysone is present at varying concentrations throughout development, cells respond to the ecdysone signaling differentially by expressing unique EcR isoforms temporally. Our recent work demonstrated temporal expression of EcR in Type II NSCs around 55h ALH mediates early to late transition in mid-larval stages<sup>15</sup>. While most animals show the complete loss of dFB neurons, in some animals, we observed a few surviving neurons that are defective in morphology and mistarget to the ectopic layers of the FB (Figure 3F-

H'). These data show that EcR acts in Type II NSCs to regulate dFB fate via E93 and might also play essential roles in axonal targeting to the proper FB layers. The FB layers express unique ligand combinations that regulate proper targeting<sup>138</sup>; one likely possibility is that EcR regulates the layer-specific expression of cell adhesion molecules or the receptors for the cell adhesion molecules within the neurons. More studies are needed to show the mechanism of how EcR and ecdysone signaling regulates CX development.

How does E93 regulate cell fate? Ecdysone-induced protein E93 regulates various developmental processes, from wing disc growth to NSC apoptosis<sup>110,119,139–142</sup>. In the developing wing discs, E93 acts as a chromatin remodeler and activates or represses genes by opening and closing chromatin<sup>141</sup>. Further work on identifying E93 targets will help identify the mechanism of E93 function in Type II NSCs. The dFB number did not increase upon the misexpression of E93 in young NSCs, indicating that E93 is not sufficient to specify dFB neurons from the young NSCs. Possibly, a combination of TFs might be required to confer dFB fate. Interestingly, in our misexpression experiments, other Type II lineages did not generate dFB neurons, indicating the role of an unknown spatial factor specific to DL1 NSCs. It is possible that ectopically expressed E93 cannot function in the young NSCs and can only act in the later periods after EcR expression. Previous studies<sup>141</sup> in *Drosophila* wing discs have shown that not all genomic targets respond to a precocious expression of E93 at all stages, suggesting that temporal factors might be required. We speculate that temporal hormonal signaling might change the chromatin landscape of the late Type II NSCs—as a result, the early/late factors have differential access to the chromatin and thus specify fate by different genes. It will be interesting to investigate the targets of the EcR and E93 in the Type II NSCs and the dFB neurons. In the post-mitotic neurons, E93 might be regulating a battery of effector genes required for consolidating and maintaining dFB neuronal identity, similar to the terminal selector genes<sup>143–145</sup>. The terminal selector genes regulate the expression of effector genes, and an overlap of unique effector genes endows neurons with distinct anatomical and functional properties. Ecdysone and E93 regulate various developmental processes in insects<sup>110,119,142,146</sup>; it will be intriguing to investigate whether E93 regulates the development of tangential input neurons in other insect species.

## Hormonal regulation of sleep behavior

How do developmental hormonal cues specify sleep behavior? Previous studies have reported the role of ecdysone signaling in regulating adult sleep behavior<sup>147–149</sup>. Whole animal ecdysone and EcR hypomorph mutants show adult sleep pattern defects<sup>147,148</sup>. Recently, EcR expression in the cortex glia was also shown to be important in regulating sleep architecture<sup>149</sup>. Our data point to an essential role of developmental hormonal signaling in adult sleep in a cell-type-specific manner via generation of 23E10+ sleep neurons. While evidence over the past decade supports a role for these cells in sleep<sup>50–53,58</sup>, more recent studies suggest that inhibition of these cells has no impact on daily sleep duration in mature adulthood<sup>55,92</sup> and raise the possibility that the sleep-promoting effect of 23E10+ neuronal activation resides in cells outside the brain<sup>91,92</sup>. Our developmental manipulations contribute further to the apparent complexity of the CX in sleep regulation. E93 knockdown in Type II NSCs causes gross abnormalities in dFB development and morphology while sparing 23E10+ VNC neurons. While mature adult sleep duration is largely intact, sleep consolidation is disturbed, multiple measures of juvenile sleep are impaired, and sleep rebound is abnormal (less consolidated). We propose that the dFB does indeed contain sleep relevant neurons, but not necessarily with a general role in daily sleep control during mature adulthood. Rather, this sleep region of the brain appears to be relevant in conditions when the drive to sleep is heightened, such as in early life or after sleep deprivation. These findings underscore how detailed insights into sleep circuit lineages and development can inform adult sleep regulatory mechanisms.

## Acknowledgments:

The authors thank Chris Doe, Doe lab, and Neural Diversity Lab members for their valuable feedback and discussions. Chris Doe and Asif Bakshi for providing critical feedback on the manuscript. We are grateful to Tzumin Lee, Chris Doe, Claude Desplan, Cheng-Yu Lee, and Gerry Rubin for sharing the reagents. Stocks obtained from the Bloomington Drosophila Stock Center (NIH P40OD018537) were used in this study. The monoclonal nc82 antibody was obtained from the Developmental Studies Hybridoma Bank, created by the NICHD of the NIH and maintained at The University of Iowa, Department of Biology, Iowa City, IA 52242. We thank UNM Biology cell biology core for providing the confocal microscopy facility. Company of Biologists Travelling Fellowship to

A.R.W, Arnold O. Beckman Postdoctoral Fellowship to J.I-B. The research was supported by NIH DP2NS111996, NIH R01NS120979 to M.S.K and through National Science Foundation CAREER Award IOS-2047020 and Sloan Research Fellowship to M.H.S.

### **Author contributions:**

Conceptualization, A.R.W., M.S.K., and M.H.S.; methodology, A. R. W performed all genetics, anatomy experiments, and confocal imaging with help from G.M.C. K.P performed initial sleep experiments; B. C and J.L performed sleep behavior experiments under the supervision of O.S. and M.S.K.; J. I-B provided the FLPStop2.0 construct and helped design the strategy to generate EcR-FLPStop2.0 flies.; visualization, A.W, M.S.K., and M.H.S.; writing-original draft, A.W, M.H.S; editing, A.W, B.C, M.S.K., and M.H.S.; funding acquisition, M.S.K., and M.H.S.; and supervision, M.S.K., and M.H.S.

### **Declaration of interests**

The authors declare no competing interests.

### **References**

1. Kohwi, M., and Doe, C.Q. (2013). Temporal Fate Specification and Neural Progenitor Competence During Development. *Nat. Rev. Neurosci.* **14**, 823–838.
2. Molnár, Z., Clowry, G.J., Šestan, N., Alzu’bi, A., Bakken, T., Hevner, R.F., Hüppi, P.S., Kostović, I., Rakic, P., Anton, E.S., et al. (2019). New insights into the development of the human cerebral cortex. *J. Anat.* **235**, 432–451. 10.1111/joa.13055.
3. Oberst, P., Agirman, G., and Jabaudon, D. (2019). Principles of progenitor temporal patterning in the developing invertebrate and vertebrate nervous system. *Curr. Opin. Neurobiol.* **56**, 185–193. 10.1016/j.conb.2019.03.004.
4. El-Danaf, R.N., Rajesh, R., and Desplan, C. (2023). Temporal regulation of neural diversity in *Drosophila* and vertebrates. *Semin. Cell Dev. Biol.* **142**, 13–22. 10.1016/j.semcd.2022.05.011.
5. Malin, J., and Desplan, C. (2021). Neural specification, targeting, and circuit formation during visual system assembly. *Proc. Natl. Acad. Sci.* **118**. 10.1073/pnas.2101823118.
6. Doe, C.Q. (2017). Temporal Patterning in the *Drosophila* CNS. *Annu. Rev. Cell Dev. Biol.* *Annu Rev Cell Dev Biol* **33**, 219–240. 10.1146/annurev-cellbio-111315.
7. Hamid, A., Gutierrez, A., Munroe, J., and Syed, M.H. (2022). The Drivers of Diversity: Integrated genetic and hormonal cues regulate neural diversity. *Semin. Cell Dev. Biol.*, S1084-9521(22)00236-1. 10.1016/j.semcd.2022.07.007.

8. Koo, B., Lee, K.-H., Ming, G., Yoon, K.-J., and Song, H. (2023). Setting the clock of neural progenitor cells during mammalian corticogenesis. *Semin. Cell Dev. Biol.* *142*, 43–53. 10.1016/j.semcdb.2022.05.013.
9. Sen, S.Q., Chanchani, S., Southall, T.D., and Doe, C.Q. (2019). Neuroblast-specific open chromatin allows the temporal transcription factor, Hunchback, to bind neuroblast-specific loci. *eLife* *8*. 10.7554/eLife.44036.
10. Sen, S.Q. (2023). Generating neural diversity through spatial and temporal patterning. *Semin. Cell Dev. Biol.* *142*, 54–66. 10.1016/j.semcdb.2022.06.002.
11. Erclik, T., Li, X., Courgeon, M., Bertet, C., Chen, Z., Baumert, R., Ng, J., Koo, C., Arain, U., Behnia, R., et al. (2017). Integration of temporal and spatial patterning generates neural diversity. *Nature* *541*, 365–370. 10.1038/nature20794.
12. Chen, Y.-C., and Konstantinides, N. (2022). Integration of Spatial and Temporal Patterning in the Invertebrate and Vertebrate Nervous System. *Front. Neurosci.* *16*.
13. Guillemot, F. (2007). Spatial and temporal specification of neural fates by transcription factor codes. *Development* *134*, 3771–3780. 10.1242/dev.006379.
14. Isshiki, T., Pearson, B., Holbrook, S., and Doe, C.Q. (2001). Drosophila neuroblasts sequentially express transcription factors which specify the temporal identity of their neuronal progeny. *Cell* *106*, 511–521.
15. Syed, M.H., Mark, B., and Doe, C.Q. (2017). Steroid hormone induction of temporal gene expression in Drosophila brain neuroblasts generates neuronal and glial diversity. *eLife* *6*, e26287. 10.7554/eLife.26287.
16. Li, X., Erclik, T., Bertet, C., Chen, Z., Voutev, R., Venkatesh, S., Morante, J., Celik, A., and Desplan, C. (2013). Temporal patterning of Drosophila medulla neuroblasts controls neural fates. *Nature* *498*, 456–462. 10.1038/nature12319.
17. Ren, Q., Yang, C.-P., Liu, Z., Sugino, K., Mok, K., He, Y., Ito, M., Nern, A., Otsuna, H., and Lee, T. (2017). Stem Cell-Intrinsic, Seven-up-Triggered Temporal Factor Gradients Diversify Intermediate Neural Progenitors. *Curr. Biol.* *27*, 1303–1313. 10.1016/j.cub.2017.03.047.
18. Liu, Z., Yang, C.-P., Sugino, K., Fu, C.-C., Liu, L.-Y., Yao, X., Lee, L.P., and Lee, T. (2015). Opposing intrinsic temporal gradients guide neural stem cell production of varied neuronal fates. *Science* *350*, 317–320. 10.1126/science.aad1886.
19. Maurange, C., Cheng, L., and Gould, A.P. (2008). Temporal Transcription Factors and Their Targets Schedule the End of Neural Proliferation in Drosophila. *Cell* *133*, 891–902. 10.1016/j.cell.2008.03.034.
20. Alsio, J.M., Tarchini, B., Cayouette, M., and Livesey, F.J. (2013). Ikaros promotes early-born neuronal fates in the cerebral cortex. *Proc. Natl. Acad. Sci.* *110*, E716–E725. 10.1073/pnas.1215707110.

21. Elliott, J., Jolicoeur, C., Ramamurthy, V., and Cayouette, M. (2008). Ikaros Confers Early Temporal Competence to Mouse Retinal Progenitor Cells. *Neuron* 60, 26–39. 10.1016/j.neuron.2008.08.008.
22. Mattar, P., Jolicoeur, C., Dang, T., Shah, S., Clark, B.S., and Cayouette, M. (2021). A Casz1–NuRD complex regulates temporal identity transitions in neural progenitors. *Sci. Rep.* 11, 3858. 10.1038/s41598-021-83395-7.
23. Dias, J.M., Alekseenko, Z., Applequist, J.M., and Ericson, J. (2014). Tgf $\beta$  Signaling Regulates Temporal Neurogenesis and Potency of Neural Stem Cells in the CNS. *Neuron* 84, 927–939. 10.1016/j.neuron.2014.10.033.
24. Telley, L., Agirman, G., Prados, J., Amberg, N., Fièvre, S., Oberst, P., Bartolini, G., Vitali, I., Cadilhac, C., Hippenmeyer, S., et al. (2019). Temporal patterning of apical progenitors and their daughter neurons in the developing neocortex. *Science* 364, eaav2522. 10.1126/science.aav2522.
25. Sagner, A., Zhang, I., Watson, T., Lazaro, J., Melchionda, M., and Briscoe, J. (2021). A shared transcriptional code orchestrates temporal patterning of the central nervous system. *PLoS Biol.* 19, e3001450. 10.1371/journal.pbio.3001450.
26. Lodato, S., and Arlotta, P. (2015). Generating Neuronal Diversity in the Mammalian Cerebral Cortex. *Annu. Rev. Cell Dev. Biol.* 31, 699–720. 10.1146/annurev-cellbio-100814-125353.
27. Sagner, A., and Briscoe, J. (2019). Establishing neuronal diversity in the spinal cord: a time and a place. *Development* 146, dev182154. 10.1242/dev.182154.
28. Honkanen, A., Adden, A., Freitas, J. da S., and Heinze, S. (2019). The insect central complex and the neural basis of navigational strategies. *J. Exp. Biol.* 222. 10.1242/jeb.188854.
29. Pfeiffer, K., and Homberg, U. (2014). Organization and Functional Roles of the Central Complex in the Insect Brain. *Annu. Rev. Entomol.* 59, 165–184. 10.1146/annurev-ento-011613-162031.
30. Turner-Evans, D.B., and Jayaraman, V. (2016). The insect central complex. *Curr. Biol.* 26, R453–R457. 10.1016/j.cub.2016.04.006.
31. Seelig, J.D., and Jayaraman, V. (2015). Neural dynamics for landmark orientation and angular path integration. *Nature* 521, 186–191. 10.1038/nature14446.
32. Lu, J., Behbahani, A.H., Hamburg, L., Westeinde, E.A., Dawson, P.M., Lyu, C., Maimon, G., Dickinson, M.H., Druckmann, S., and Wilson, R.I. (2022). Transforming representations of movement from body- to world-centric space. *Nature* 601, 98–104. 10.1038/s41586-021-04191-x.
33. Lyu, C., Abbott, L.F., and Maimon, G. (2022). Building an allocentric travelling direction signal via vector computation. *Nature* 601, 92–97. 10.1038/s41586-021-04067-0.

34. Fisher, Y.E. (2022). Flexible navigational computations in the *Drosophila* central complex. *Curr. Opin. Neurobiol.* 73, 102514. 10.1016/j.conb.2021.12.001.
35. Turner-Evans, D.B., Jensen, K.T., Ali, S., Paterson, T., Sheridan, A., Ray, R.P., Wolff, T., Lauritzen, J.S., Rubin, G.M., Bock, D.D., et al. (2020). The Neuroanatomical Ultrastructure and Function of a Biological Ring Attractor. *Neuron* 108, 145-163.e10. 10.1016/j.neuron.2020.08.006.
36. Hulse, B.K., Haberkern, H., Franconville, R., Turner-Evans, D.B., Takemura, S.-Y., Wolff, T., Noorman, M., Dreher, M., Dan, C., Parekh, R., et al. (2021). A connectome of the *Drosophila* central complex reveals network motifs suitable for flexible navigation and context-dependent action selection. *eLife* 10, e66039. 10.7554/eLife.66039.
37. Heinze, S., Narendra, A., and Cheung, A. (2018). Principles of Insect Path Integration. *Curr. Biol.* 28, R1043–R1058. 10.1016/j.cub.2018.04.058.
38. Dacke, M., Baird, E., el Jundi, B., Warrant, E.J., and Byrne, M. (2021). How Dung Beetles Steer Straight. *Annu. Rev. Entomol.* 66, 243–256. 10.1146/annurev-ento-042020-102149.
39. Collett, M., Chittka, L., and Collett, T.S. (2013). Spatial Memory in Insect Navigation. *Curr. Biol.* 23, R789–R800. 10.1016/j.cub.2013.07.020.
40. Sayre, M.E., Templin, R., Chavez, J., Kempenaers, J., and Heinze, S. (2021). A projectome of the bumblebee central complex. *eLife* 10, e68911. 10.7554/eLife.68911.
41. Strauss, R. (2002). The central complex and the genetic dissection of locomotor behaviour. *Curr. Opin. Neurobiol.* 12, 633–638.
42. Strausfeld, N.J. (1999). Chapter 24 A Brain Region in Insects That Supervises Walking. In *Progress in Brain Research Peripheral and Spinal Mechanisms in the Neural Control of Movement.*, M. D. Binder, ed. (Elsevier), pp. 273–284. 10.1016/S0079-6123(08)62863-0.
43. Martin, J.R., Raabe, T., and Heisenberg, M. (1999). Central complex substructures are required for the maintenance of locomotor activity in *Drosophila melanogaster*. *J. Comp. Physiol. [A]* 185, 277–288. 10.1007/s003590050387.
44. Strauss, R., and Heisenberg, M. (1993). A higher control center of locomotor behavior in the *Drosophila* brain. *J. Neurosci.* 13, 1852–1861. 10.1523/JNEUROSCI.13-05-01852.1993.
45. Bender, J.A., Pollack, A.J., and Ritzmann, R.E. (2010). Neural activity in the central complex of the insect brain is linked to locomotor changes. *Curr. Biol. CB* 20, 921–926. 10.1016/j.cub.2010.03.054.
46. Martin, J.P., Guo, P., Mu, L., Harley, C.M., and Ritzmann, R.E. (2015). Central-complex control of movement in the freely walking cockroach. *Curr. Biol. CB* 25, 2795–2803. 10.1016/j.cub.2015.09.044.
47. Sareen, P.F., McCurdy, L.Y., and Nitabach, M.N. (2021). A neuronal ensemble encoding adaptive choice during sensory conflict in *Drosophila*. *Nat. Commun.* 12, 4131. 10.1038/s41467-021-24423-y.

48. Musso, P.-Y., Junca, P., and Gordon, M.D. (2021). A neural circuit linking two sugar sensors regulates satiety-dependent fructose drive in *Drosophila*. *Sci. Adv.* 7, eabj0186. 10.1126/sciadv.abj0186.
49. Ni, J.D., Gurav, A.S., Liu, W., Ogunmowo, T.H., Hackbart, H., Elsheikh, A., Verdegaal, A.A., and Montell, C. (2019). Differential regulation of the *Drosophila* sleep homeostat by circadian and arousal inputs. *eLife* 8, e40487. 10.7554/eLife.40487.
50. Donlea, J.M., Thimgan, M.S., Suzuki, Y., Gottschalk, L., and Shaw, P.J. (2011). Inducing sleep by remote control facilitates memory consolidation in *Drosophila*. *Science* 332, 1571–1576. 10.1126/science.1202249.
51. Pimentel, D., Donlea, J.M., Talbot, C.B., Song, S.M., Thurston, A.J.F., and Miesenböck, G. (2016). Operation of a homeostatic sleep switch. *Nature* 536, 333–337.
52. Donlea, J.M., Pimentel, D., and Miesenböck, G. (2014). Neuronal Machinery of Sleep Homeostasis in *Drosophila*. *Neuron* 81, 860–872. 10.1016/j.neuron.2013.12.013.
53. Donlea, J.M., Pimentel, D., Talbot, C.B., Kempf, A., Omoto, J.J., Hartenstein, V., and Miesenböck, G. (2018). Recurrent Circuitry for Balancing Sleep Need and Sleep. *Neuron* 97, 378–389.e4. 10.1016/j.neuron.2017.12.016.
54. Kayser, M.S., Yue, Z., and Sehgal, A. (2014). A critical period of sleep for development of courtship circuitry and behavior in *Drosophila*. *Science* 344, 269–274.
55. Gong, N.N., Luong, H.N.B., Dang, A.H., Mainwaring, B., Shields, E., Schmeckpeper, K., Bonasio, R., and Kayser, M.S. (2022). Intrinsic maturation of sleep output neurons regulates sleep ontogeny in *Drosophila*. *Curr. Biol. CB* 32, 4025–4039.e3. 10.1016/j.cub.2022.07.054.
56. Chakravarti Dilley, L., Szuperak, M., Gong, N.N., Williams, C.E., Saldana, R.L., Garbe, D.S., Syed, M.H., Jain, R., and Kayser, M.S. (2020). Identification of a molecular basis for the juvenile sleep state. *eLife* 9, e52676. 10.7554/eLife.52676.
57. Liu, Q., Liu, S., Kodama, L., Driscoll, M.R., and Wu, M.N. (2012). Two Dopaminergic Neurons Signal to the Dorsal Fan-Shaped Body to Promote Wakefulness in *Drosophila*. *Curr. Biol.* 22, 2114–2123. 10.1016/j.cub.2012.09.008.
58. Ueno, T., Tomita, J., Tanimoto, H., Endo, K., Ito, K., Kume, S., and Kume, K. (2012). Identification of a dopamine pathway that regulates sleep and arousal in *Drosophila*. *Nat. Neurosci.* 15, 1516–1523. 10.1038/nn.3238.
59. Liu, S., Liu, Q., Tabuchi, M., Wu Correspondence, M.N., and Wu, M.N. (2016). Sleep Drive Is Encoded by Neural Plastic Changes in a Dedicated Circuit Synaptic plasticity within a dedicated neural circuit encodes sleep pressure in *Drosophila* and provides a mechanistic explanation for the generation and persistence of sleep drive. *Sleep Drive Is Encoded by Neural Plastic Changes in a Dedicated Circuit*. *Cell* 165, 1347–1360. 10.1016/j.cell.2016.04.013.
60. Shafer, O.T., and Keene, A.C. (2021). The Regulation of *Drosophila* Sleep. *Curr. Biol.* 31, R38–R49. 10.1016/j.cub.2020.10.082.

61. Wolff, T., Iyer, N.A., and Rubin, G.M. (2015). Neuroarchitecture and neuroanatomy of the *Drosophila* central complex: A GAL4-based dissection of protocerebral bridge neurons and circuits: *Drosophila Central Complex Anatomy and Neurons*. *J. Comp. Neurol.* 523, 997–1037. 10.1002/cne.23705.
62. Hanesch, U., Fischbach, K.-F., and Heisenberg, M. (1989). Neuronal architecture of the central complex in *Drosophila melanogaster*. *Cell Tissue Res.* 257, 343–366. 10.1007/BF00261838.
63. Yu, H.-H., Awasaki, T., Schroeder, M.D., Long, F., Yang, J.S., He, Y., Ding, P., Kao, J.-C., Wu, G.Y.-Y., Peng, H., et al. (2013). Clonal development and organization of the adult *Drosophila* central brain. *Curr. Biol. CB* 23, 633–643. 10.1016/j.cub.2013.02.057.
64. Yang, J.S., Awasaki, T., Yu, H.-H., He, Y., Ding, P., Kao, J.-C., and Lee, T. (2013). Diverse neuronal lineages make stereotyped contributions to the *Drosophila* locomotor control center, the central complex. *J. Comp. Neurol.* 521, 2645–2662. 10.1002/cne.23339.
65. Bayraktar, O.A., and Doe, C.Q. (2013). Combinatorial temporal patterning in progenitors expands neural diversity. *Nature* 498, 449–455. 10.1038/nature12266.
66. Izergina, N., Balmer, J., Bello, B., and Reichert, H. (2009). Postembryonic development of transit amplifying neuroblast lineages in the *Drosophila* brain. *Neural Develop.* 4, 44. 10.1186/1749-8104-4-44.
67. Viktorin, G., Riebli, N., Popkova, A., Giangrande, A., and Reichert, H. (2011). Multipotent neural stem cells generate glial cells of the central complex through transit amplifying intermediate progenitors in *Drosophila* brain development. *Dev. Biol.* 356, 553–565. 10.1016/j.ydbio.2011.06.013.
68. Ito, M., Masuda, N., Shinomiya, K., Endo, K., and Ito, K. (2013). Systematic analysis of neural projections reveals clonal composition of the *Drosophila* brain. *Curr. Biol. CB* 23, 644–655. 10.1016/j.cub.2013.03.015.
69. Bello, B.C., Izergina, N., Caussinus, E., and Reichert, H. (2008). Amplification of neural stem cell proliferation by intermediate progenitor cells in *Drosophila* brain development. *Neural Develop.* 3, 5. 10.1186/1749-8104-3-5.
70. Boone, J.Q., and Doe, C.Q. (2008). Identification of *Drosophila* type II neuroblast lineages containing transit amplifying ganglion mother cells. *Dev. Neurobiol.* 68, 1185–1195. 10.1002/dneu.20648.
71. Bowman, S.K., Rolland, V., Betschinger, J., Kinsey, K.A., Emery, G., and Knoblich, J.A. (2008). The Tumor Suppressors Brat and Numb Regulate Transit-Amplifying Neuroblast Lineages in *Drosophila*. *Dev. Cell* 14, 535–546. 10.1016/j.devcel.2008.03.004.
72. Wang, Y.-C., Yang, J.S., Johnston, R., Ren, Q., Lee, Y.-J., Luan, H., Brody, T., Odenwald, W.F., and Lee, T. (2014). *Drosophila* intermediate neural progenitors produce lineage-dependent related series of diverse neurons. *Development* 141, 253–258. 10.1242/dev.103069.

73. Pebworth, M.-P., Ross, J., Andrews, M., Bhaduri, A., and Kriegstein, A.R. (2021). Human intermediate progenitor diversity during cortical development. *Proc. Natl. Acad. Sci.* **118**. 10.1073/pnas.2019415118.
74. Florio, M., and Huttner, W.B. (2014). Neural progenitors, neurogenesis and the evolution of the neocortex. *Development* **141**, 2182–2194. 10.1242/dev.090571.
75. Fietz, S.A., Kelava, I., Vogt, J., Wilsch-Bräuninger, M., Stenzel, D., Fish, J.L., Corbeil, D., Riehn, A., Distler, W., Nitsch, R., et al. (2010). OSVZ progenitors of human and ferret neocortex are epithelial-like and expand by integrin signaling. *Nat. Neurosci.* **13**, 690–699. 10.1038/nn.2553.
76. Hansen, D.V., Lui, J.H., Parker, P.R.L., and Kriegstein, A.R. (2010). Neurogenic radial glia in the outer subventricular zone of human neocortex. *Nature* **464**, 554–561. 10.1038/nature08845.
77. Boyan, G.S., and Reichert, H. (2011). Mechanisms for complexity in the brain: generating the insect central complex. *Trends Neurosci.* **34**, 247–257. 10.1016/j.tins.2011.02.002.
78. Boyan, G., and Liu, Y. (2014). Timelines in the insect brain: fates of identified neural stem cells generating the central complex in the grasshopper *Schistocerca gregaria*. *Dev. Genes Evol.* **224**, 37–51. 10.1007/s00427-013-0462-8.
79. Ludwig, P., Williams, J. I. d., Lodde, E., Reichert, H., and Boyan, G.S. (1999). Neurogenesis in the median domain of the embryonic brain of the grasshopper *Schistocerca gregaria*. *J. Comp. Neurol.* **414**, 379–390. 10.1002/(SICI)1096-9861(19991122)414:3<379::AID-CNE7>3.0.CO;2-5.
80. Boyan, G.S., and Williams, J.L.D. (1997). Embryonic development of the pars intercerebralis/central complex of the grasshopper. *Dev. Genes Evol.* **207**, 317–329. 10.1007/s004270050119.
81. Williams, J.L.D., and Boyan, G.S. (2008). Building the central complex of the grasshopper *Schistocerca gregaria*: axons pioneering the w, x, y, z tracts project onto the primary commissural fascicle of the brain. *Arthropod Struct. Dev.* **37**, 129–140. 10.1016/j.asd.2007.05.005.
82. Boyan, G., Liu, Y., Khalsa, S.K., and Hartenstein, V. (2017). A conserved plan for wiring up the fan-shaped body in the grasshopper and *Drosophila*. *Dev. Genes Evol.* **227**, 253–269. 10.1007/s00427-017-0587-2.
83. Farnworth, M.S., Eckermann, K.N., and Bucher, G. (2020). Sequence heterochrony led to a gain of functionality in an immature stage of the central complex: A fly–beetle insight. *PLOS Biol.* **18**, e3000881. 10.1371/journal.pbio.3000881.
84. Farnworth, M.S., Bucher, G., and Hartenstein, V. (2022). An atlas of the developing *Tribolium castaneum* brain reveals conservation in anatomy and divergence in timing to *Drosophila melanogaster*. *J. Comp. Neurol.* 10.1002/cne.25335.
85. Keene, A.C., and Duboue, E.R. (2018). The origins and evolution of sleep. 10.1242/jeb.159533.

86. Helfrich-Förster, C. (2018). Sleep in Insects. *Annu. Rev. Entomol.* 63, 69–86. 10.1146/annurev-ento-020117-043201.
87. Qian, Y., Cao, Y., Deng, B., Yang, G., Li, J., Xu, R., zhang, D., Huang, J., and Rao, Y. (2017). Sleep homeostasis regulated by 5HT2b receptor in a small subset of neurons in the dorsal fan-shaped body of drosophila. *eLife* 6, e26519. 10.7554/eLife.26519.
88. Wiggin, T.D., and Griffith, L.C. (2023). Subtype-Specific Roles of Ellipsoid Body Ring Neurons in Sleep Regulation in Drosophila. *J. Neurosci.* 43, 764–786. 10.1523/JNEUROSCI.1350-22.2022.
89. Tomita, J., Ban, G., Kato, Y.S., and Kume, K. (2021). Protocerebral Bridge Neurons That Regulate Sleep in *Drosophila melanogaster*. *Front. Neurosci.* 15, 647117. 10.3389/fnins.2021.647117.
90. Singh, P., Aleman, A., Omoto, J.J., Nguyen, B.-C., Kandimalla, P., Hartenstein, V., and Donlea, J.M. (2023). Examining sleep modulation by *Drosophila* ellipsoid body neurons. *eNeuro*. 10.1523/ENEURO.0281-23.2023.
91. Jones, J.D., Holder, B.L., Eiken, K.R., Vogt, A., Velarde, A.I., Elder, A.J., McEllin, J.A., and Dissel, S. (2023). Regulation of sleep by cholinergic neurons located outside the central brain in *Drosophila*. *PLOS Biol.* 21, e3002012. 10.1371/journal.pbio.3002012.
92. De, J., Wu, M., Lambatan, V., Hua, Y., and Joiner, W.J. (2023). Re-examining the role of the dorsal fan-shaped body in promoting sleep in *Drosophila*. *Curr. Biol.* 33, 3660–3668.e4. 10.1016/j.cub.2023.07.043.
93. Shaw, P.J., Cirelli, C., Greenspan, R.J., and Tononi, G. (2000). Correlates of Sleep and Waking in *Drosophila melanogaster*. *Science* 287, 1834–1837. 10.1126/science.287.5459.1834.
94. Roffwarg, H.P., Muzio, J.N., and Dement, W.C. (1966). Ontogenetic development of the human sleep-dream cycle. *Science* 152, 604–619. 10.1126/science.152.3722.604.
95. Doldur-Balli, F., Imamura, T., Veatch, O.J., Gong, N.N., Lim, D.C., Hart, M.P., Abel, T., Kayser, M.S., Brodkin, E.S., and Pack, A.I. (2022). Synaptic dysfunction connects autism spectrum disorder and sleep disturbances: A perspective from studies in model organisms. *Sleep Med. Rev.* 62, 101595. 10.1016/j.smrv.2022.101595.
96. Robinson-Shelton, A., and Malow, B.A. (2015). Sleep Disturbances in Neurodevelopmental Disorders. *Curr. Psychiatry Rep.* 18, 6. 10.1007/s11920-015-0638-1.
97. Baker, E.K., and Richdale, A.L. (2015). Sleep Patterns in Adults with a Diagnosis of High-Functioning Autism Spectrum Disorder. *Sleep* 38, 1765–1774. 10.5665/sleep.5160.
98. Angriman, M., Caravale, B., Novelli, L., Ferri, R., and Bruni, O. (2015). Sleep in children with neurodevelopmental disabilities. *Neuropediatrics* 46, 199–210. 10.1055/s-0035-1550151.
99. Abel, E.A., and Tonnsen, B.L. (2017). Sleep phenotypes in infants and toddlers with neurogenetic syndromes. *Sleep Med.* 38, 130–134. 10.1016/j.sleep.2017.07.014.

100. Veatch, O.J., Maxwell-Horn, A.C., and Malow, B.A. (2015). Sleep in Autism Spectrum Disorders. *Curr. Sleep Med. Rep.* 1, 131–140. 10.1007/s40675-015-0012-1.
101. Kandimalla, P., Omoto, J.J., Hong, E.J., and Hartenstein, V. (2023). Lineages to circuits: the developmental and evolutionary architecture of information channels into the central complex. *J. Comp. Physiol. A.* 10.1007/s00359-023-01616-y.
102. Ren, Q., Awasaki, T., Huang, Y.-F., Liu, Z., and Lee, T. (2016). Cell Class-Lineage Analysis Reveals Sexually Dimorphic Lineage Compositions in the Drosophila Brain. *Curr. Biol.* 26, 2583–2593. 10.1016/j.cub.2016.07.086.
103. Lee, T. (2017). Wiring the Drosophila Brain with Individually Tailored Neural Lineages. *Curr. Biol. CB* 27, R77–R82.
104. Homem, C.C.F., and Knoblich, J.A. (2012). Drosophila neuroblasts: a model for stem cell biology. *Development* 139, 4297–4310. 10.1242/dev.080515.
105. Syed, M.H., Mark, B., and Doe, C.Q. (2017). Playing Well with Others: Extrinsic Cues Regulate Neural Progenitor Temporal Identity to Generate Neuronal Diversity. *Trends Genet. TIG* 33, 933-942 10.1016/j.tig.2017.08.005.
106. Ito, K., and Hotta, Y. (1992). Proliferation pattern of postembryonic neuroblasts in the brain of *Drosophila melanogaster*. *Dev. Biol.* 149, 134–148. 10.1016/0012-1606(92)90270-q.
107. Truman, J.W., and Bate, M. (1988). Spatial and temporal patterns of neurogenesis in the central nervous system of *Drosophila melanogaster*. *Dev. Biol.* 125, 145–157.
108. Truman, J.W., Schuppe, H., Shepherd, D., and Williams, D.W. (2004). Developmental architecture of adult-specific lineages in the ventral CNS of *Drosophila*. *Dev. Camb. Engl.* 131, 5167–5184. 10.1242/dev.01371.
109. Prokop, A., and Technau, G.M. (1991). The origin of postembryonic neuroblasts in the ventral nerve cord of *Drosophila melanogaster*. *Dev. Camb. Engl.* 111, 79–88. 10.1242/dev.111.1.79.
110. Truman, J.W., and Riddiford, L.M. (2019). The evolution of insect metamorphosis: a developmental and endocrine view. *Philos. Trans. R. Soc. B Biol. Sci.* 374, 20190070. 10.1098/rstb.2019.0070.
111. Truman, J.W., and Riddiford, L.M. (2023). Drosophila postembryonic nervous system development: a model for the endocrine control of development. *Genetics*, iyac184. 10.1093/genetics/iyac184.
112. Dumstrei, K., Wang, F., Nassif, C., and Hartenstein, V. (2003). Early development of the *Drosophila* brain: V. Pattern of postembryonic neuronal lineages expressing DE-cadherin. *J. Comp. Neurol.* 455, 451–462. 10.1002/cne.10484.
113. Yaniv, S.P., and Schuldiner, O. (2016). A fly's view of neuronal remodeling. *Wiley Interdiscip. Rev. Dev. Biol.* 5, 618–635. 10.1002/wdev.241.

114. Truman, J.W., Price, J., Miyares, R.L., and Lee, T. (2023). Metamorphosis of memory circuits in *Drosophila* reveals a strategy for evolving a larval brain. *eLife* 12, e80594. 10.7554/eLife.80594.
115. Lee, K., and Doe, C.Q. (2021). A locomotor neural circuit persists and functions similarly in larvae and adult *Drosophila*. *eLife* 10, e69767. 10.7554/eLife.69767.
116. Andrade, I.V., Riebli, N., Nguyen, B.-C.M., Omoto, J.J., Cardona, A., and Hartenstein, V. (2019). Developmentally Arrested Precursors of Pontine Neurons Establish an Embryonic Blueprint of the *Drosophila* Central Complex. *Curr. Biol.* 29, 412-425.e3. 10.1016/J.CUB.2018.12.012.
117. Riebli, N., Viktorin, G., and Reichert, H. (2013). Early-born neurons in type II neuroblast lineages establish a larval primordium and integrate into adult circuitry during central complex development in *Drosophila*. *Neural Develop.* 8, 6. 10.1186/1749-8104-8-6.
118. Postembryonic lineages of the *Drosophila* brain: II. Identification of lineage projection patterns based on MARCM clones (2013). *Dev. Biol.* 384, 258–289. 10.1016/J.YDBIO.2013.07.009.
119. Truman, J.W. (2019). The Evolution of Insect Metamorphosis. *Curr. Biol.* 29, R1252–R1268. 10.1016/j.cub.2019.10.009.
120. Yamanaka, N., Rewitz, K.F., and O'Connor, M.B. (2013). Ecdysone Control of Developmental Transitions: Lessons from *Drosophila* Research. *Annu. Rev. Entomol.* 58, 497–516. 10.1146/annurev-ento-120811-153608.
121. Thummel, C.S. (2001). Molecular mechanisms of developmental timing in *C. elegans* and *Drosophila*. *Dev. Cell* 1, 453–465.
122. Truman, J.W., Talbot, W.S., Fahrbach, S.E., and Hogness, D.S. (1994). Ecdysone receptor expression in the CNS correlates with stage-specific responses to ecdysteroids during *Drosophila* and *Manduca* development. *Dev. Camb. Engl.* 120, 219–234. 10.1242/dev.120.1.219.
123. Handler, A.M. (1982). Ecdysteroid titers during pupal and adult development in *Drosophila melanogaster*. *Dev. Biol.* 93, 73–82. 10.1016/0012-1606(82)90240-8.
124. Fisher, Y.E., Yang, H.H., Isaacman-Beck, J., Xie, M., Gohl, D.M., and Clandinin, T.R. (2017). FlpStop, a tool for conditional gene control in *Drosophila*. *eLife* 6, e22279. 10.7554/eLife.22279.
125. Isaacman-Beck, J., Paik, K.C., Wienecke, C.F.R., Yang, H.H., Fisher, Y.E., Wang, I.E., Ishida, I.G., Maimon, G., Wilson, R.I., and Clandinin, T.R. (2020). SPARC enables genetic manipulation of precise proportions of cells. *Nat. Neurosci.* 23, 1168–1175. 10.1038/s41593-020-0668-9.
126. Cherbas, L., Hu, X., Zhimulev, I., Belyaeva, E., and Cherbas, P. (2003). EcR isoforms in *Drosophila*: testing tissue-specific requirements by targeted blockade and rescue. *Dev. Camb. Engl.* 130, 271–284. 10.1242/dev.00205.

127. McGuire, S.E., Mao, Z., and Davis, R.L. (2004). Spatiotemporal Gene Expression Targeting with the TARGET and Gene-Switch Systems in *Drosophila*. *Sci. STKE* 2004, pl6–pl6. [10.1126/stke.2202004pl6](https://doi.org/10.1126/stke.2202004pl6).
128. Wiggin, T.D., Goodwin, P.R., Donelson, N.C., Liu, C., Trinh, K., Sanyal, S., and Griffith, L.C. (2020). Covert sleep-related biological processes are revealed by probabilistic analysis in *Drosophila*. *Proc. Natl. Acad. Sci.* 117, 10024–10034. [10.1073/pnas.1917573117](https://doi.org/10.1073/pnas.1917573117).
129. Xu, X., Yang, W., Tian, B., Sui, X., Chi, W., Rao, Y., and Tang, C. (2021). Quantitative investigation reveals distinct phases in *Drosophila* sleep. *Commun. Biol.* 4, 1–11. [10.1038/s42003-021-01883-y](https://doi.org/10.1038/s42003-021-01883-y).
130. Hendricks, J.C., Finn, S.M., Panckeri, K.A., Chavkin, J., Williams, J.A., Sehgal, A., and Pack, A.I. (2000). Rest in *Drosophila* Is a Sleep-like State. *Neuron* 25, 129–138. [10.1016/S0896-6273\(00\)80877-6](https://doi.org/10.1016/S0896-6273(00)80877-6).
131. Alphen, B. van, Yap, M.H.W., Kirszenblat, L., Kottler, B., and Swinderen, B. van (2013). A Dynamic Deep Sleep Stage in *Drosophila*. *J. Neurosci.* 33, 6917–6927. [10.1523/JNEUROSCI.0061-13.2013](https://doi.org/10.1523/JNEUROSCI.0061-13.2013).
132. Chowdhury, B., Abhilash, L., Ortega, A., Liu, S., and Shafer, O. (2022). Homeostatic control of deep sleep in *Drosophila*: Implications for Discovering Correlates of Sleep Pressure. [2022.09.30.510368](https://doi.org/10.1101/2022.09.30.510368). [10.1101/2022.09.30.510368](https://doi.org/10.1101/2022.09.30.510368).
133. Niki, A., A.I., T.-H.L., Hang, L., Eleni, N., Qiongyi, Z., Trent, P., Philip, B., J, S.P., and Bruno, van S. (2023). Experimentally induced active and quiet sleep engage non-overlapping transcriptomes in *Drosophila*. *eLife* 12. [10.7554/eLife.88198](https://doi.org/10.7554/eLife.88198).
134. Abhilash, L., and Shafer, O.T. (2023). A two-process model of *Drosophila* sleep reveals an inter-dependence between circadian clock speed and the rate of sleep pressure decay. [2022.08.12.503775](https://doi.org/10.1101/2022.08.12.503775). [10.1101/2022.08.12.503775](https://doi.org/10.1101/2022.08.12.503775).
135. Hamid, A., Gattuso, H., Caglar, A.N., Pillai, M., Steele, T., Gonzalez, A., Nagel, K., and Syed, M. (2023). The RNA-binding protein Imp specifies olfactory navigation circuitry and behavior in *Drosophila*. [2023.05.26.542522](https://doi.org/10.1101/2023.05.26.542522). [10.1101/2023.05.26.542522](https://doi.org/10.1101/2023.05.26.542522).
136. Jain, S., Lin, Y., Kurmangaliyev, Y.Z., Valdes-Aleman, J., LoCascio, S.A., Mirshahidi, P., Parrington, B., and Zipursky, S.L. (2022). A global timing mechanism regulates cell-type-specific wiring programmes. *Nature* 603, 112–118. [10.1038/s41586-022-04418-5](https://doi.org/10.1038/s41586-022-04418-5).
137. Sakamura, S., Hsu, F.-Y., Tsujita, A., Abubaker, M.B., Chiang, A.-S., and Matsuno, K. (2023). Ecdysone signaling determines lateral polarity and remodels neurites to form *Drosophila*'s left-right brain asymmetry. *Cell Rep.*, 112337. [10.1016/j.celrep.2023.112337](https://doi.org/10.1016/j.celrep.2023.112337).
138. Xie, X., Tabuchi, M., Corver, A., Duan, G., Wu, M.N., and Kolodkin, A.L. (2019). Semaphorin 2b Regulates Sleep-Circuit Formation in the *Drosophila* Central Brain. *Neuron* 104, 322–337.e14. [10.1016/j.neuron.2019.07.019](https://doi.org/10.1016/j.neuron.2019.07.019).

139. Pahl, M.C., Doyle, S.E., and Siegrist, S.E. (2019). E93 Integrates Neuroblast Intrinsic State with Developmental Time to Terminate MB Neurogenesis via Autophagy. *Curr. Biol.* **29**, 750–762.e3. 10.1016/J.CUB.2019.01.039.
140. Lam, G., Nam, H.-J., Velentzas, P.D., Baehrecke, E.H., and Thummel, C.S. (2022). Drosophila E93 promotes adult development and suppresses larval responses to ecdysone during metamorphosis. *Dev. Biol.* **481**, 104–115. 10.1016/j.ydbio.2021.10.001.
141. Mou, X., Duncan, D.M., Baehrecke, E.H., and Duncan, I. (2012). Control of target gene specificity during metamorphosis by the steroid response gene E93. *Proc. Natl. Acad. Sci.* **109**, 2949–2954. 10.1073/pnas.1117559109.
142. Ureña, E., Manjón, C., Franch-Marro, X., and Martín, D. (2014). Transcription factor E93 specifies adult metamorphosis in hemimetabolous and holometabolous insects. *Proc. Natl. Acad. Sci. U. S. A.* **111**, 7024–7029. 10.1073/pnas.1401478111.
143. Hobert, O. (2021). Homeobox genes and the specification of neuronal identity. *Nat. Rev. Neurosci.* **22**, 627–636. 10.1038/s41583-021-00497-x.
144. Sun, H., and Hobert, O. (2023). Temporal transitions in the postembryonic nervous system of the nematode *Caenorhabditis elegans*: Recent insights and open questions. *Semin. Cell Dev. Biol.* **142**, 67–80. 10.1016/j.semcd.2022.05.029.
145. Sun, H., and Hobert, O. (2021). Temporal transitions in the post-mitotic nervous system of *Caenorhabditis elegans*. *Nature* **600**, 93–99. 10.1038/s41586-021-04071-4.
146. Fernandez-Nicolas, A., Machaj, G., Ventos-Alfonso, A., Pagone, V., Minemura, T., Ohde, T., Daimon, T., Ylla, G., and Belles, X. (2023). Reduction of embryonic E93 expression as a hypothetical driver of the evolution of insect metamorphosis. *Proc. Natl. Acad. Sci.* **120**, e2216640120. 10.1073/pnas.2216640120.
147. Ishimoto, H., and Kitamoto, T. (2010). The Steroid Molting Hormone Ecdysone Regulates Sleep in Adult *Drosophila melanogaster*. *Genetics* **185**, 269–281. 10.1534/genetics.110.114587.
148. Ishimoto, H., Lark, A.R.S., and Kitamoto, T. (2012). Factors that Differentially Affect Daytime and Nighttime Sleep in *Drosophila melanogaster*. *Front. Neurol.* **3**, 10.3389/fneur.2012.00024.
149. Li, Y., Haynes, P., Zhang, S.L., Yue, Z., and Sehgal, A. (2023). Ecdysone acts through cortex glia to regulate sleep in *Drosophila*. *eLife* **12**, e81723. 10.7554/eLife.81723.
150. Powsner, L. (1935). The Effects of Temperature on the Durations of the Developmental Stages of *Drosophila melanogaster*. *Physiological Zoology* **8**, 474–520. 10.1086/physzool.8.4.30151263.
151. Perrotta, A.T., and Been, M.D. (1991). A pseudoknot-like structure required for efficient self-cleavage of hepatitis delta virus RNA. *Nature* **350**, 434–436. 10.1038/350434a0.
152. Nagarkar-Jaiswal, S., Lee, P.-T., Campbell, M.E., Chen, K., Anguiano-Zarate, S., Cantu Gutierrez, M., Busby, T., Lin, W.-W., He, Y., Schulze, K.L., et al. (2015). A library of

MiMICs allows tagging of genes and reversible, spatial and temporal knockdown of proteins in *Drosophila*. *eLife* 4, e05338. 10.7554/eLife.05338.

153. Geissmann, Q., Rodriguez, L.G., Beckwith, E.J., and Gilestro, G.F. (2019). Rethomics: An R framework to analyse high-throughput behavioural data. *PLOS ONE* 14, e0209331. 10.1371/journal.pone.0209331.

## Methods

### Experimental Model and Subject Details

All flies (*Drosophila melanogaster*) were maintained on conventional Bloomington Food formulation at ~25°C, ~65% relative humidity, and under a 12-hour light/dark cycle (lights on at 7 AM) throughout development and adulthood unless otherwise stated. The egg-laying for RNAi and FLPStop experiments was performed at 25°C, and then hatched larvae were transferred and allowed to develop at 29°C until adult stages. Also, standardized age matching conversions were used for Gal80<sup>ts</sup> experiments: 18°C is 2.25X slower than 25°C, and 29°C is 1.03X faster than 25°C<sup>150</sup>. The genotype information of the flies used in each experiment is listed in the Key resource table.

For knocking down E93 in NSCs, we initially used E93 RNAi (from the VDRC stock center) along with UAS Dicer, and the phenotype we observed was severe. Later, we used the same E93 RNAi without dicer, and a similar phenotype was observed. We used a second E93 RNAi from the BDSC stock center, which also gave a similar phenotype.

### Method Details

#### Immunostaining

Fly brains from L3 larvae or 5–7-day old adult flies were dissected in ice-cold insect media (Schneiders media) (Sigma Aldrich) and fixed in 4% paraformaldehyde (PFA) (EMS) in PBST (1X phosphate-buffered saline with 0.5 % Triton X-100) for 27 min at room temperature. Following fixing, three 20-minute washes in 1X PBST were performed, and brains were blocked for 40

minutes in blocking solution PBST containing 2.5% Normal Goat serum and 2.5% Normal Donkey Serum (Jackson ImmunoResearch) at room temperature. After blocking, brain samples were incubated with primary antibody at 4°C overnight for larvae and two nights for adult brains. Brains were rinsed and washed thrice for 20 minutes in PBST and then incubated with secondary antibody for 2 hours at room temperature for larvae brains and for adult brains for two nights 4°C. After the secondary antibody, brains were rinsed again, and three 20-min PBST washes were performed. After antibody staining, DPX mounting was performed on brain samples. For DPX mounting, the protocol from Janelia FlyLight was followed.

The dilutions for various primary antibodies are as Chicken anti-GFP (1:1500), Rat anti-Dpn (1:500), Rabbit anti-Asense (1:500), Mouse anti- Bruchpilot (nc82) (1:50), Mouse anti-EcR-B1 (1:2000), Rabbit anti-mCherry (1:500), Guinea Pig anti-E93 (1:300).

### **Confocal imaging, data acquisition, and image analysis**

Fluorescent image stacks of whole-mount fly brains were taken using a Zeiss LSM 780 confocal microscope. In the figures, only slices corresponding to the FB neuropil (stained with nc82) were shown, giving an exact idea about the axonal targeting of dFB neurons in CX. For dFB neurons stained with GFP, the slices that give the full projection of these neurons were shown. Fiji cell counter plug-in performed adult brain cell counting, and statistical analysis (Student's T test, one-way ANOVA) was done in Graph Pad prism. Figures were processed and assembled in Adobe Photoshop and Adobe Illustrator, respectively. Asterisks indicate levels of significant differences (\*: p<0.05, \*\*: p<0.01, \*\*\*: p<0.001, \*\*\*\*: p<0.0001).

### **Clonal Analysis and Birthdating**

The CLIn fly females and cell class-specific males were allowed to mate in a bottle and then shifted to an egg-laying cage. The egg laying was done on apple agar caps. The eggs were allowed to hatch at 25°C. Then newly hatched larvae 0-3.5hr old were manually collected and reared on food caps (at 25°C) until the desired time point. For lineage mapping of cell class-specific neurons, larvae were heat shocked at 37°C at Zero ALH. The zero ALH heat shock (for lineage determination) duration was determined and customized to get only one NSC clone one time. The most effective heat shock time was 10-12 minutes at 37 °C to get individual NSC clones. The individual NSC clones obtained were compared to an already available source<sup>64</sup>. For temporal birth dating the neurons from a particular cell class lineage, the 50-minute heat shock was performed at 0h, 48h, and 76h ALH. The larvae were transferred to undergo normal development at 25°C and dissected as adults. Both male and female adult flies were dissected in our experiments.

### **Generation of FlpStop2.0 plasmid for transgenesis**

The original FlpStop1.0 was generated to allow for conditional gene control in *Drosophila*<sup>124</sup>. For some genes, for unknown reasons, the FlpStop1.0 cassette did not abrogate expression of the transcript in the presence of FLP Recombinase, though the authors speculated about potential readthrough of transcriptional and translational stop sequences<sup>124</sup>. The FlpStop2.0 cassette was updated to include a 10x repeated sequence of the self-cleaving ribozyme from the Hepatitis Delta

Virus (HDV)<sup>151</sup> (Figure 3A). In other molecular constructs, this sequence has been shown to effectively disrupt transcription and expression of transgenes<sup>125</sup>.

The pFlpStop2.0-attB-UAS-2.1-tdTom plasmid was generated through the synthesis of the FlpStop 2.0 cassette (Figure 3A) and molecular cloning into the FlpStop-attB-UAS-2.1-tdTom<sup>124</sup> by Genscript (Piscataway, NJ, USA). Constructs were sequence-verified by single primer extension (Sequetech; Mountain View, CA) and were submitted to Addgene. Transgenic flies harboring the FlpStop 2.0 cassette generated through injection of the plasmid and insertion within an intron of the Ecdysone Receptor, as described below.

### Generation of FlpStop2.0 transgenic flies

Transgenic flies harboring the FlpStop 2.0 cassette in an intron of the Ecdysone Receptor (EcR) were generated via standard construct injection (~50ng plasmid) by Bestgene (Chino Hills, CA, USA). The MiMIC strain<sup>152</sup> used for injection was *y*[1] *w*[\*]; Mi{*y*[+mDint2]=MIC}EcR[MI05320] (Bloomington Drosophila Stock Center Stock 38619). 4 transgenic lines were identified through the loss of *y* and were PCR-tested for orientation of insertion by Bestgene. We then tested these lines for expression of TdTomato and gene disruption after conditional expression of FLP Recombinase (Figure S3A-D). The transgenic line for conditional disruption of EcR was isolated and has been maintained.

### Sleep assays

Sleep behavior was measured using the Drosophila Activity Monitoring (DAM) system (Trikinetics, Waltham MA). Single-beam DAM2 monitors were used for sleep deprivation experiments, and multi-beam DAM5H monitors were used for all other sleep experiments. Newly eclosed male flies from crosses were collected and aged in group housing on standard food. Flies were then anesthetized on CO<sub>2</sub> pads and loaded into glass tubes (70mm x 5mm x 3mm) containing 5% sucrose and 2% agar medium. Juvenile adult flies were loaded at ~ZT6 on the day of eclosion; mature adult flies were loaded at the same time but after aging for 6-8 days. To deprive flies of sleep, mechanical shaking stimulus was applied by attaching DAM2 monitors to microplate adapters on vortexers (VWR). Monitors were shaken for 2 seconds randomly within every 20-second window for 12 hours during ZT12 – ZT24. Activity counts were collected every minute, and periods of inactivity lasting at least 5 minutes were classified as sleep; for long sleep bout analysis, only inactivity lasting at least 60 minutes was counted. Sleep parameters were analyzed with a custom R script using Rethomics package<sup>153</sup>.

### Key Resource Table

REAGENT or RESOURCE	SOURCE	IDENTIFIER
<b>Antibodies</b>		
nc82 (anti-Bruchpilot) anti-Mouse	DSHB	Cat#AB_2314866 RRID:AB_2314866

Monoclonal Anti-GFP Chicken	Aves Labs	Cat#GFP-1010 RRID:AB_2307313
Anti-mCherry Polyclonal Rabbit	Novus Biologicals	Cat#NBP2-25157 RRID:AB_2753204
Monoclonal Anti-Dpn Rat	Abcam	Cat#11D1BC7 RRID:AB_2687586
Anti-Asense Rabbit	Cheng-Yu Lee	N/A
Anti-E93 Guinea Pig	Chris Doe	N/A
Anti-EcR-B1 Mouse	Carl Thummel	N/A
Alexa Flour 647 Anti-Mouse	Jackson ImmunoResearch	Cat#715-605-151 RRID:AB_2340863
Alexa Flour 647 Anti-Rabbit	Jackson ImmunoResearch	
Alexa Flour 488 Anti-Chicken	Jackson ImmunoResearch	Cat#703-545-155 RRID:AB_2340375
Alexa Flour 555 Anti-Rabbit	Invitrogen	Cat#A-21429 RRID:AB_2535850
Alexa Flour 555 Anti-Rat	Jackson ImmunoResearch	
Dylight 405 Anti-Guinea Pig	Jackson ImmunoResearch	Cat#706-475-148 RRID:AB_2340470
Normal Donkey Serum	Jackson ImmunoResearch	Cat#017-000-121 RRID:AB_2337258
Normal Goat Serum	Jackson ImmunoResearch	Cat#005-000-121 RRID:AB_2336990
Chemicals, peptides, and recombinant proteins		
16% Paraformaldehyde	Electron Microscopy Sciences	Cat#15710
Triton X-100	Sigma-Aldrich	Cat#T8787
Apple Juice	S. Martinelli & Co	N/A
Schneider's Insect medium	Sigma-Aldrich	Cat#S0146
Agar	Sigma-Aldrich	Cat#A1296
DPX mounting medium	Sigma-Aldrich	Cat#06522
Sucrose	Research products International	Cat#57-50-1
Xylene	Fisher Scientific	Cat#1330-20-7, 100-41-4
Experimental models: Strains of <i>Drosophila melanogaster</i>		
23E10-LexA on II	BDSC	RRID:BDSC_52693
23E10-GAL4 on III	BDSC	RRID:BDSC_49032

Pointed-GAL4 on III	Yuh-Nung Jan	N/A
UAS-Dicer (on X Chromosome)	BDSC	RRID:BDSC_58756
UAS-E93RNAi on II	BDSC	RRID:BDSC_57868
UAS-E93RNAi on II	VDRC	104390
UAS-E93HA III	Fly ORF	F000587
LexAopmCD8GFP on III	BDSC	RRID:BDSC_32207
UAS-KKRNAi on II	VDRC	60103
Worniu-GAL4, Ase-GAL80 on II	Chris Doe	N/A
UAS-FLPPEST on X	BDSC	RRID:BDSC_24644
UAS-mCherryRNAi on III	BDSC	RRID:BDSC_35785
Sco/Cyo ; TubGAL80 <sup>ts</sup>	BDSC	RRID:BDSC_7018
LexAopFRTstopFRTGFP on III	BDSC	RRID:BDSC_57588
W <sup>1118</sup>	BDSC	RRID:BDSC_5905
Hs-ATG>KOT>FLP, dpn>FRT-stop-FRT>Cre:PEST; actin^LoxP-GAL80-stopLoxP^LexAP65, LexAop-rCD2RFP-p10-spacer-UAS-mCD8GFP-p10; stg14-KD	Tzumin Lee Lab	N/A
23E10-LexA; Pointed-GAL4, LexAop-mCD8GFP	This Study	N/A
UAS-Dicer; UAS-E93RNAi	This study	N/A
UAS-Dicer; UAS-KKRNAi	This study	N/A
UAS-E93RNAi; TubGAL80 <sup>ts</sup>	This study	N/A
UAS-FLPPEST; Wor-GAL4, Ase- GAL80; LexAop-FRTstopFRT-mcD8GFP	This study	N/A
UAS-FLP, ActinFRTstopFRTGAL4; EcRFLPStop2.0/ Cyo	This study	N/A
EcRFLPStop2.0/ Cyo	This Study	N/A
UAS-E93-HA	Fly ORF	F000587
UAS-EcR-DN	BDSC	RRID:BDSC_6872
UAS-EcR-B1	BDSC	RRID:BDSC_6469
Software and Algorithms		
ImageJ	Fiji	Version: 2.9.0/1.53t
Adobe Photoshop (v24.1.1)	Adobe Systems	<a href="https://www.adobe.com/products/photoshop.html">https://www.adobe.com/products/photoshop.html</a>
Adobe Illustrator (v27.2)	Adobe Systems	<a href="https://www.adobe.com/products/illustrator.html">https://www.adobe.com/products/illustrator.html</a>
GraphPad Prism 9	GraphPad Software	<a href="https://www.graphpad.com/">https://www.graphpad.com/</a>
R Studio		<a href="https://www.rstudio.com">https://www.rstudio.com</a>

Other		
Drosophila Activity Monitoring system	Trikinetics	Single-beam DAM system, DAM5H multibeam system

### Fly Genotypes with Associated Figures

Experimental Line	Main	Supplementary
Wor-GAL4, Ase-GAL80; UAS- FLP PEST; LexAop-FRTstopFRT- mCD8GFP crossed to 23E10-LexA	Figure 1C	
hs-ATG>KOT>FLP, dpn>FRT-stop- FRT>Cre:PEST; actin^LoxP-GAL80- stopLoxP^LexAP65, lexAop-rCD2RFP- p10-spacer-UAS-mCD8GFP-p10; stg14-KD crossed to 23E10-GAL4	Figure 2C, 2D, 2E, 2F and 2G.	
23E10-LexA/Cyo; Pointed-GAL4, LexAop-mCD8GFP /MKRS To EcRFLPStop2.0/Cyo	Figure 3C, 3C' and 3F,3F'	Figure 3S 3 A, A'
23E10-LexA/Cyo; Pointed-GAL4, LexAopm-CD8GFP /MKRS To UAS- FLP, ActinFRTstopFRTGAL4 ; EcR FLPStop2.0/ Cyo	Figure 3D, 3D' and 3G,3G'	Figure 3S 3 B, B'
23E10-LexA/Cyo; Pointed-GAL4, LexAop-mCD8GFP/ MKRS To UAS- EcR-DN	3E, 3E' and 3H, 3H'	
Pointed-GAL4 To EcRFLPStop2.0/Cyo		3S 1 A, A'
Pointed-GAL4 To UAS-FLP, ActinFRTstopFRTGAI4 ; EcR FLPStop2.0/ Cyo		3S 1 B, B'
23E10-LexA ; Pointed-GAL4, LexAop- mCD8GFP		3S 2 A, A'
23E10-LexA ; Pointed-GAL4, LexAop- mCD8GFP To UAS-EcRB1		3S 2 B, B'
23E10-GAL4, UAS-mCD8GFP	Figure 4A, 4A', 4A''	
23E10LexA/Cyo; Pointed GAL4, LexAop-mCD8GFP/MKRS To UAS-Dicer; UAS-KKRNAi/Cyo	Figure 4B, 4B'	4S 3 A, A', A''

23E10-LexA/Cyo; Pointed-GAL4, LexAop-mCD8GFP/MKRS To UAS-Dicer; UAS-E93RNAi/Cyo	Figure 4C, 4C'	4S 3 B, B', B''
23E10-LexA/Cyo; Pointed-GAL4, LexAop-mCD8GFP/MKRS To UAS-E93-HA	Figure 4D, 4D'	4S 3 C, C', C''
UAS-Dicer; Pointed-GAL4 To UAS-KKRNAi		4S 1 A
UAS-Dicer; Pointed-GAL4 To UAS-E93RNAi		4S 1 B
23E10-LexA/Cyo; Pointed- GAL4, LexAop-mCD8GFP/MKRS To UAS-mCherryRNAi		4S 2 A, A'
23E10-LexA/Cyo; Pointed- GAL4, LexAop-mCD8GFP/MKRS To UAS-E93RNAi (BDSC)		4S 2 B, B'
23E10-LexA/Cyo; Pointed-GAL4, LexAop-mCD8GFP/MKRS To UAS-E93RNAi; TubGAL80ts	Figure 5 C, C', D, D', E, E' and F, F'	
W1118 to UAS-E93RNAi	Figure 6	6S 1
Pointed-GAL4 to UAS-KKRNAi	Figure 6	6S 1
Pointed-GAL4 to UAS-E93RNAi	Figure 6	6S 1
23E10LexA/Cyo; Pointed GAL4, LexAop-mCD8GFP/MKRS To UAS-Dicer; UAS-KKRNAi/Cyo		6S 2 A, A'
23E10-LexA/Cyo; Pointed-GAL4, LexAop-mCD8GFP/MKRS To UAS-Dicer; UAS-E93RNAi/Cyo		6S 2 B, B'